PPARγ and NOTCH Regulate Regional Identity in the Murine Cardiac Outflow Tract

Mayyasa Rammah, Magali Théveniau-Ruissy, Rachel Sturny, Francesca Rochais, Robert Kelly

PPARγ and NOTCH Regulate Regional Identity in the Murine Cardiac Outflow Tract

Mayyasa Rammah,* Magali Théveniau-Ruissy,* Rachel Sturny, Francesca Rochais,† Robert G. Kelly†

BACKGROUND: The arterial pole of the heart is a hotspot for life-threatening forms of congenital heart defects (CHDs). Development of this cardiac region occurs by addition of Second Heart Field (SHF) progenitor cells to the embryonic outflow tract (OFT) and subsequently the base of the ascending aorta and pulmonary trunk. Understanding the cellular and genetic mechanisms driving arterial pole morphogenesis is essential to provide further insights into the cause of CHDs.

METHODS: A synergistic combination of bioinformatic analysis and mouse genetics as well as embryo and explant culture experiments were used to dissect the cross-regulatory transcriptional circuitry operating in future subaortic and subpulmonary OFT myocardium.

RESULTS: Here, we show that the lipid sensor PPARγ (peroxisome proliferator–activated receptor gamma) is expressed in future subpulmonary myocardium in the inferior wall of the OFT and that PPARγ signaling-related genes display regionalized OFT expression regulated by the transcription factor TBX1 (T-box transcription factor 1). Modulating PPARγ activity in ex vivo cultured embryos treated with a PPARγ agonist or antagonist or deleting *Pparγ* in cardiac progenitor cells using *Mesp1-Cre* reveals that *Pparγ* is required for addition of future subpulmonary myocardium and normal arterial pole development. Additionally, the non-canonical DLK1 (delta-like noncanonical Notch ligand 1)/NOTCH (Notch receptor 1)/HES1 (Hes family bHLH transcription factor 1) pathway negatively regulates *Pparγ* in future subaortic myocardium in the superior OFT wall.

CONCLUSIONS: Together these results identify *Pparγ* as a regulator of regional transcriptional identity in the developing heart, providing new insights into gene interactions involved in congenital heart defects.

GRAPHIC ABSTRACT: A graphic abstract is available for this article.

Key Words: aorta ■ heart defects, congenital ■ morphogenesis ■ myocardium ■ PPAR gamma

The arterial pole or outlet of the heart, which comprises the myocardial base of the ascending aorta and pulmonary trunk, is an important component of the definitive heart and a hotspot for life-threatening forms of congenital heart defects (CHDs). The arterial pole of the heart is formed by progressive addition of myocardial cells to the outflow tract (OFT) from Second Heart Field (SHF) progenitor cells.[1,2] Located in the adjacent pharyngeal mesoderm, SHF cells contribute to major parts of the heart including right ventricular, OFT, and atrial myocardium.[3–5] Direct or indirect perturbations of SHF deployment result in impaired embryonic OFT development and lead to a large spectrum of arterial pole defects including common arterial trunk, double outlet right ventricle, tetralogy of Fallot, and transposition of the great arteries, accounting for more than 30% of human CHDs.[6,7] Understanding the cellular and genetic mechanisms driving arterial pole morphogenesis is, therefore, essential to provide further insights into the cause of CHDs.

Studies from our laboratory and others have revealed that subaortic and subpulmonary myocardium, which are prefigured in the superior and inferior regions of

Correspondence to: Francesca Rochais, PhD, Aix Marseille Univ, INSERM, Marseille Medical Genetics, Faculté de Médecine de la Timone, 27 boulevard Jean Moulin 13005 Marseille, France. Email francesca.rochais@univ-amu.fr or Robert G. Kelly, PhD, Aix Marseille University, CNRS UMR 7288, IBDM, Campus de Luminy, Case 907, 13009, Marseille, France, Email robert.kelly@univ-amu.fr
*M. Rammah and M. Théveniau-Ruissy contributed equally
† F. Rochais and R.G. Kelly contributed equally as last authors

Novelty and Significance

What Is Known?

- Development of the arterial pole of the heart occurs by the addition of Second Heart Field progenitor cells from the pharyngeal mesoderm to the outflow tract (OFT).
- The base of the ascending aorta and pulmonary trunk are prefigured in the superior and inferior OFT, respectively, displaying distinct genetic signatures.
- *Hes family bHLH transcription factor 1* (*Hes1*) and *T-box transcription factor 1* (*Tbx1*) encode transcription factors required for arterial pole development.
- *Peroxisome proliferator–activated receptor gamma* (*Pparγ*) is enriched in the inferior OFT.

What New Information Does This Article Contribute?

- PPARγ signaling controls cross-regulatory transcriptional programs in the OFT.
- *Pparγ* is required for the addition of early Second Heart Field cells to the OFT.
- *Pparγ* expression in the inferior OFT is *Tbx1*-dependent.
- The NOTCH (Notch receptor 1)/Hes1 pathway controls the molecular identity of the superior OFT through repressing *Pparγ* expression.
- *Delta-like 1 (Dlk1)*, a non-canonical NOTCH ligand and PPARγ antagonist, is expressed in the superior OFT and regulates OFT transcriptional domains.

We provide insights into the regulatory pathways operating in distinct OFT subdomains during mammalian heart development. We show that *Pparγ* is expressed in the *Tbx1*-dependent inferior OFT wall and is required for normal arterial pole development. We demonstrate that *Pparγ* expression is repressed by NOTCH/HES1 signaling in the superior wall of the OFT and identify DLK1 (delta-like noncanonical Notch ligand 1) as an upstream NOTCH/HES1 signaling regulator in the superior OFT wall. Together these findings contribute to our understanding of the complex regulatory interactions controlling regional identity in the OFT and the origins of congenital heart defects.

Nonstandard Abbreviations and Acronyms

AHF	anterior heart field
CHDs	congenital heart defects
Cre	cyclization recombinase
DLK1	delta-like noncanonical Notch ligand 1
E	embryonic day
HES1	Hes family bHLH transcription factor 1
Hoxb1	homeobox B1
iOFT	inferior wall of the OFT
IPA	Ingenuity Pathway Analysis
MAPK/ERK	mitogen-activated kinase protein/extracellular regulated MAP kinase
Mef2c	Myocyte-specific enhancer factor 2C
MESP1	mesoderm posterior 1
MF20	Myosin Heavy Chain antibody
NICD1	Notch intracellular domain
NOTCH	Notch receptor 1
OFT	outflow tract
PH3	phospho-histone 3
PPAR	peroxisome proliferator–activated receptor
PPARGC1A	peroxisome proliferator–activated receptor gamma coactivator 1-alpha
PPARγ/α/δ	peroxisome proliferator–activated receptor gamma/alpha/delta
PPRE	peroxisome proliferator response element
PREF1	Pre-adipocyte factor 1
rDLK1	recombinant DLK1
RT-qPCR	quantitative reverse transcription polymerase chain reaction
SHF	Second Heart Field
sOFT	superior wall of the OFT
TBX1	T-box transcription factor 1

the embryonic OFT, respectively, display transcriptional differences.[5,8–13] For example, the *y96-Myf5-nlacZ-16 Sema3c* enhancer trap transgene is expressed in the inferior wall of the OFT (iOFT) and subsequently at the base of the pulmonary trunk, whereas the *A17-Myf5-nlacZ-T55 Hes1* enhancer trap transgene (*Hes1-Tg*) is expressed in the superior wall of the OFT (sOFT) and later in the myocardium at the base of the ascending aorta.[9,10,14] Moreover, retrospective clonal analysis of OFT cardiomyocytes identified regionalized clusters of clonally related cells located in the myocardium at the base

of either the aorta or pulmonary artery, suggesting that distinct progenitor cell lineages contribute to the inferior and superior regions of the OFT.[10]

The origin of the subaortic and subpulmonary myocardial progenitor cells in the SHF is still under investigation, nevertheless, studies using lineage tracing, fluorescent dye labeling, and retrospective clonal analysis demonstrate that in addition to the anterior part of the SHF that gives rise to major parts of the OFT,[1,15] a *Hoxb1*-expressing subpopulation of the posterior SHF contributes to the iOFT and subsequently to subpulmonary myocardium.[11,16] SHF cells expressing the T-box transcription *Tbx1* have been shown to contribute to the inferior and lateral but not superior walls of the embryonic OFT.[8,17] Moreover, TBX1 (T-box transcription factor 1), by controlling the addition of *Hoxb1*-expressing cells from the posterior SHF to the iOFT, is required for the correct morphogenesis of subpulmonary myocardium in the fetal heart.[9,12] Interestingly, conditional gene ablation mouse models have demonstrated that endodermal-produced Sonic hedgehog signals also participate in the OFT morphogenesis by regulating SHF progenitor cell survival and subpulmonary OFT development.[18,19] In contrast, lineage tracing of *Wnt11*-expressing cells identified a specific SHF subpopulation that contributes to the sOFT and subsequently to cardiomyocytes at the base of the aorta.[20] The transcriptional repressor and main target of the NOTCH (Notch receptor 1) signaling pathway, *Hes1*, is expressed in future subaortic myocardium, and *Hes1* loss of function results in arterial pole and ventricular septal defects.[14] Recent analysis of a tamoxifen-inducible Cre (cyclization recombinase) line driven by the *Mef2c-AHF* enhancer indicates that these distinct progenitor cell populations make temporally sequential contributions to the elongating OFT, subaortic myocardium preceding addition of subpulmonary cells.[21] The superior and inferior myocardial walls of the early OFT are thus prefigured in the SHF. However, the spatial localization of these progenitor cells and the regulatory networks driving the distinct transcriptional signatures of OFT subdomains remain to be determined.

Using microarray-based gene expression profiling, we previously identified peroxisome proliferator–activated receptor gamma (*Pparγ*) among the most enriched genes expressed in the iOFT.[12] PPARs belong to a nuclear hormone receptor superfamily of ligand-inducible transcription factors that regulate gene expression by binding with retinoid X receptor as a heterodimeric partner to specific PPRE (peroxisome proliferator response element) DNA targets. The PPAR family comprises three genes *Pparγ*, *Pparα*, and *Pparβ/δ*, encoding receptors with distinct tissue distribution, ligand specificity, and physiological roles.[22] PPARγ plays a key role in lipogenesis and is involved in adipocyte differentiation and insulin sensitivity.[23] Global deletion of *Pparγ* leads to embryonic death at midgestation with mutant embryos displaying cardiac defects potentially due to placental dysfunction.[24] The role of *Pparγ* in adult cardiac structure and function has been investigated.[25] Although *Pparγ* targeted deletion in cardiomyocytes causes ventricular hypertrophy, its increased expression results in dilated cardiomyopathy associated with increased lipid and glycogen stores.[26–28] During heart development, PPARγ activity has been shown to be required for epicardial adipose tissue formation.[29] Nevertheless, the precise roles of *Pparγ* in heart morphogenesis remain to be investigated.

In this study, we demonstrate that PPARγ signaling-related genes are regionally expressed in the OFT and that the PPARγ signaling pathway is required for arterial pole development. Using mouse genetics as well as embryo and explant culture experiments we have dissected the transcriptional cross-regulatory circuitry operating in future subaortic and subpulmonary OFT myocardium. We present evidence that the DLK1 (delta-like noncanonical Notch ligand 1)/NOTCH/HES1 pathway represses *Pparγ* together with its downstream-related targets in the sOFT whereas TBX1 activates PPARγ signaling in the iOFT, implicating complementary PPARγ and non-canonical NOTCH signaling in regional transcriptional identity in the outflow tract.

METHODS

Data Availability

A detailed description of all experimental procedures and statistical tests can be found in the Supplemental Methods.

Transgenic Mouse Lines

The following mouse lines were used in this study: *Hes1*$^{+/-}$,[30] *Tbx1*$^{+/tm1Pa}$ (*Tbx1*$^{+/-}$),[31] *A17-Myf5-nlacZ-T55*,[10] *Pparγ 1*$^{fl/fl}$,[32] *Hes1*,[33] *Hoxb1*$^{IRES-Cre}$,[11] *Mef2c-AHF-Cre*,[34] *Mesp1-Cre*,[35] *Rosa26-YFP*,[36] and CD1 mice. Transgenic and mutant mice were maintained on mixed (C57Bl/6 and CD1) or inbred (FVB/N) backgrounds. The source of the animals used in this study together with their origin, background, and original publication are listed in the Major Resources Tables in the Supplemental Material. Developmental stage was determined by considering noon on the day of appearance of a copulation plug as embryonic day (E) 0.5. Genomic DNA from yolk sacs or tail biopsies was genotyped by polymerase chain reaction using primer sequences as described in the above references and reported in the Majors Resources Tables. Animal care was in accordance with national and institutional guidelines. Animals were maintained under controlled light and temperature conditions with free access to food and water. Mice were treated humanely, and all efforts were made to minimize the animals' suffering and the number of mice used in the study. For all experiments, animals were randomly allocated into experimental groups after considering their specific genotypes when this was required. No animals were excluded from this study and male and female embryos were randomly and blindly chosen for all experiments.

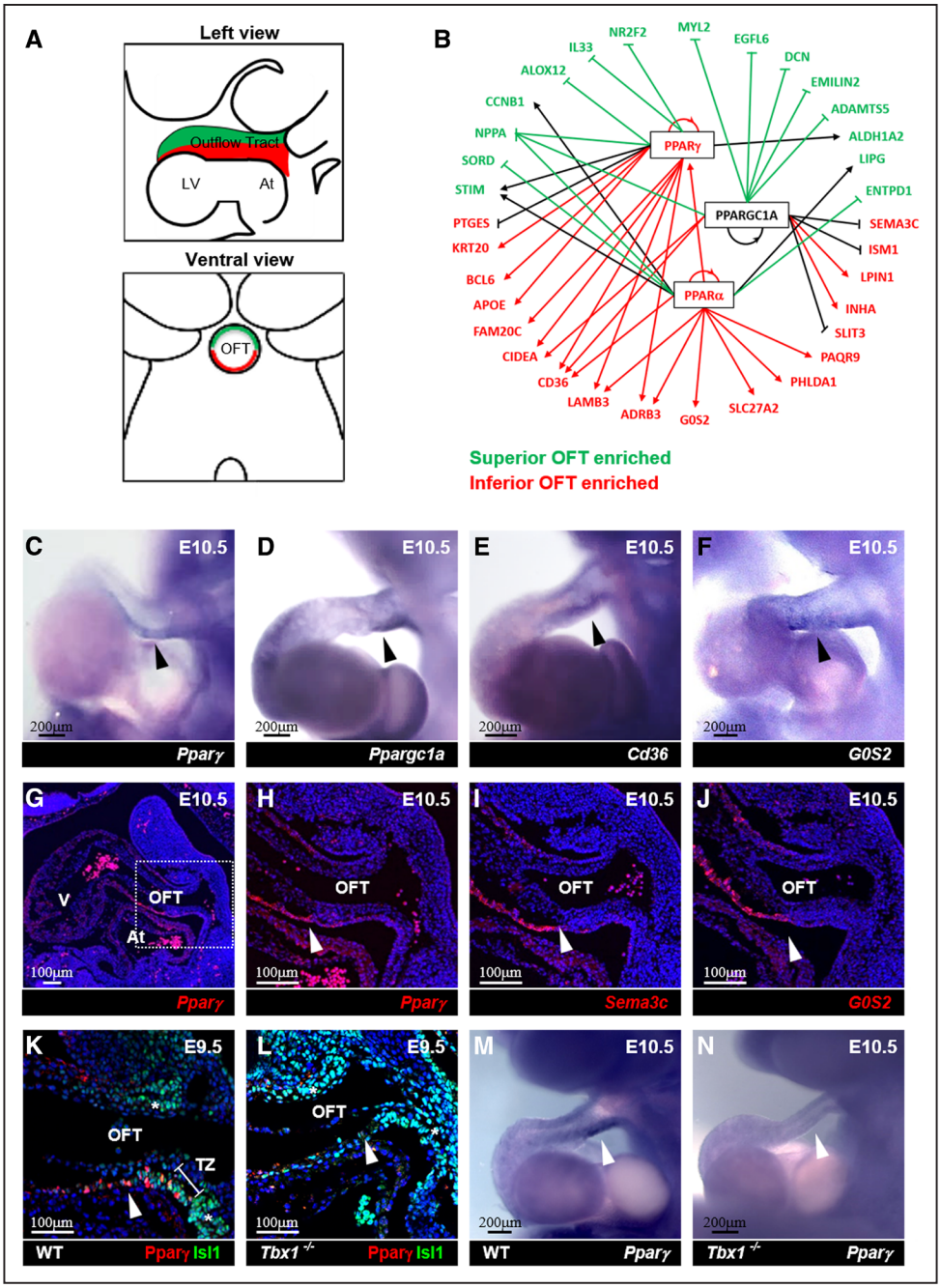

Figure 1. Ingenuity analysis on the transcriptional profile of the superior and inferior outflow tract (OFT) distinguish PPAR (peroxisome proliferator–activated receptor) signaling pathway genes.

A, Embryonic day (E) 10.5 embryo schematic left and ventral (heart removed) views showing the superior (green) and inferior (red) outflow tract (OFT). **B**, Mechanistic network showing the molecular relationship between the predicted upstream regulators PPARγ, PPARα, and PPARGC1A (peroxisome proliferator-activated receptor gamma coactivator 1-alpha) and superior and inferior OFT differentially expressed genes based on Ingenuity Knowledge Database (Fischer exact test, $P<0.05$ and Z score ≥2). PPARγ, PPARα, and PPARGC1A were predicted as upstream activator or inhibitors of inferior wall of the OFT (iOFT; red) and superior wall of the OFT (sOFT; green) enriched genes, respectively. PPARGC1A (black), did not show specific enrichment. Predicted inhibition of iOFT enriched genes or activation of sOFT enriched genes are indicated with black lines. **C–F,** Enrichment of PPAR pathway–related genes in the iOFT. Left views of E10.5 wild-type (WT) embryos after in situ hybridization for *Pparγ*(**C,** N=6), *Ppargc1a* (**D,** N=6), *Cd36* (**E,** N=8), and *G0S2* (**F,** N=3) riboprobes showing transcript enrichment in the iOFT (arrowheads). **G–J,** Sagittal sections of wild-type embryos showing the enrichment of *Pparγ* (**G** and **H,** N=4), *Sema3c* (**I,** N=3), and *G0S2* (**J**, N=3) in the iOFT at E10.5. High magnification of *Pparγ* OFT expression is shown in **H**. **K** and **L**, Immunofluorescence on sagittal sections at the level of the OFT on wild-type and *Tbx1*$^{-/-}$ E9.5 embryos. **K**, Wild-type embryo displaying localized expression of *Pparγ* in the iOFT (arrowhead) and transition zone (TZ) in ISL1 (ISLET LIM homeobox 1) positive cells (N=5). Note that *Isl1* is also expressed in the Second Heart Field and sOFT (asterisks). **L**, *Tbx1*$^{-/-}$ embryo displaying reduced OFT *Pparγ* expression (arrowhead, N=3). **M** and **N**, Left views of E10.5 embryos after whole-mount in situ hybridization with *Pparγ* riboprobe. *Pparγ* expression is reduced in the iOFT of *Tbx1*$^{-/-}$ (**N,** arrowhead, N=6) compared to wild-type (**M**, arrowhead, N=5) embryos. Presented results are representative of biological replicates. At indicates atrium; LV, left ventricle; and V, ventricle.

RESULTS

Bioinformatic Pathway Analysis Implicates PPARγ Signaling in the Transcriptional Control of Distinct Superior and Inferior OFT Domains

Using microarray-based gene expression profiling, we previously established the genetic signature of future subpulmonary and subaortic domains in the inferior and superior walls of the E10.5 mouse OFT (Figure 1A). To uncover novel genetic regulatory networks that may control subaortic and subpulmonary myocardial domains, we analyzed our dataset[12] using Ingenuity Pathway Analysis (IPA).

Mapping iOFT and sOFT enriched genes to the IPA knowledge database, signaling and metabolic pathways associated with regional OFT genetic signatures were identified. This analysis predicted that the PPAR signaling pathway is active in the iOFT, where both *Pparα* and *Pparγ* transcripts are enriched. The gene encoding PPARγ is among the most highly enriched genes

Table. List of Genes Enriched in the OFT Subdomains and Involved in the PPAR Signaling Pathway as Defined by Ingenuity Pathway Analysis

ID	Symbol	Entrez gene name	Expr log2 ratio	Expr *P* value
1420715_a_at	*PPARγ*	peroxisome proliferator–activated receptor gamma	1.331	0.002
1417812_a_at	*LAMB3*	Laminin subunit beta 3	1.169	0.00057
1420696_at	*SEMA3C*	semaphorin 3C	0.983	0.0081
1432466_a_at	*APOE*	Apolipoprotein E	0.859	0.0124
1436987_at	*ISM1*	Isthmin 1	0.795	0.00187
1450883_a_at	*CD36*	CD36 molecule	0.788	0.00597
1448700_at	*G0S2*	G0/G1 switch 2	0.77	0.02
1436168_at	*PAQR9*	Progestin and adipoQ receptor family member 9	0.675	0.00297
1421818_at	*BCL6*	BCL6 transcription repressor	0.64	0.0226
1449450_at	*PTGES*	Prostaglandin E synthase	0.622	0.00424
1455918_at	*ADRB3*	Adrenoceptor beta 3	0.608	0.0469
1416316_at	*SLC27A2*	Solute carrier family 27 member 2	0.547	0.0446
1426284_at	*KRT20*	Keratin 20	0.512	0.0197
1427086_at	*SLIT3*	Slit guidance ligand 3	0.505	0.00569
1422728_at	*INHA*	Inhibin subunit alpha	0.504	0.00181
1417956_at	*CIDEA*	Cell death inducing DFFA like effector a	0.499	0.0498
1443827_x_at	*FAM20C*	FAM20C golgi associated secretory pathway kinase	0.488	0.0134
1418288_at	*LPIN1*	Lipin 1	0.483	0.00067
1439675_at	*PPARα*	PPARα	0.456	0.0221
1418835_at	*PHLDA1*	Pleckstrin homology like domain family A member 1	0.424	0.00667
1448394_at	*MYL2*	Myosin light chain 2	−0.403	0.0127
1416076_at	*CCNB1*	Cyclin B1	−0.439	0.0292
1419332_at	*EGFL6*	EGF-like domain multiple 6	−0.447	0.00837
1422699_at	*ALOX12*	Arachidonate 12-lipoxygenase, 12S type	−0.452	0.0238
1448320_at	*STIM1*	Stromal interaction molecule 1	−0.456	0.00301
1436475_at	*NR2F2*	Nuclear receptor subfamily 2 group F member 2	−0.499	0.0121
1416200_at	*IL33*	Interleukin 33	−0.516	0.0238
1423326_at	*ENTPD1*	Ectonucleoside triphosphate diphosphohydrolase 1	−0.578	0.0246
1456404_at	*ADAMTS5*	ADAM metallopeptidase with thrombospondin type 1 motif 5	−0.629	0.044
1426584_a_at	*SORD*	Sorbitol dehydrogenase	−0.79	0.0008
1435264_at	*EMILIN2*	Elastin microfibril interfacer 2	−1.154	0.00123
1421262_at	*LIPG*	Lipase G, endothelial type	−1.169	0.0482
1422789_at	*ALDH1A2*	Aldehyde dehydrogenase 1 family member A2	−1.519	0.00806
1449368_at	*DCN*	Decorin	−1.648	0.0263
1456062_at	*NPPA*	Natriuretic peptide A	−2.208	0.0132

ADAM indicates a disintegrin and metalloproteinase; adipoQ, adiponectin; BCL, B cell lymphoma; DFFA, DNA fragmentation factor subunit alpha; EGF: Epidermal Growth Factor; FAM20C, Family with sequence similarity 20, member C; OFT, outflow tract; and PPAR, peroxisome proliferator–activated receptor.

in the iOFT (Log2 fold change=1.3, $P<0.002$) while *Pparα* transcripts present a lower enrichment (Log2 fold change=0.46, $P<0.023$) suggesting that PPARγ may act as an upstream regulator of regional transcriptional identity in the OFT (Table)[12].

Mechanistic network analysis revealed that 16 out of the 20 genes identified by IPA analysis as being in the PPAR signaling pathway and significantly enriched in the iOFT (including *Cd36, Apoe,* and *G0S2*) are predicted to be under positive regulation of PPAR transcription factors. Conversely, 11 out of the 15 PPAR signaling pathway genes significantly enriched in the sOFT (including *Nppa*) are predicted to be negatively regulated by PPAR transcription factors (Figure 1B; PPARγ [$P<0.001$, Z score>2], PPARα [$P<0.01$, Z score>2] and PPARGC1A [PPAR gamma coactivator 1-alpha; $P<0.001$, Z score>2]). PPARγ signaling may thus be involved in the genetic control of distinct inferior and superior OFT transcriptional signatures. In situ hybridization experiments were performed at E10.5 to confirm the regionalized expression of PPARγ signaling pathway–related genes in the OFT. Our results demonstrated differential expression of *Pparγ*, *Ppargc1a* as well as the downstream target genes *Cd36* and *G0S2* in the iOFT expressing *Sema3c* (Figure 1C through 1J), thus validating the IPA results and supporting a potential role for PPARγ signaling in OFT development.

We previously demonstrated the *Tbx1* dependency of gene expression in the iOFT.[12] Therefore, we investigated whether *Pparγ* expression in the developing OFT is regulated by TBX1. Immunofluorescence and in situ hybridization experiments performed on wild-type embryos at E9.5 and E10.5, respectively, confirmed that *Pparγ* expression is regionalized in the iOFT, in addition to expression in SHF progenitor cells in the dorsal pericardial wall close to the junction with the OFT, a region termed the transition zone (Figure 1K and 1M). *Pparγ* expression was not observed in the OFT or SHF of *Tbx1*$^{-/-}$ embryos (Figure 1L and 1N). Quantitative reverse transcription polymerase chain reaction (RT-qPCR) analysis performed on RNA prepared from isolated OFTs of wild-type and *Tbx1*$^{-/-}$ embryos confirmed that *Pparγ* expression is significantly reduced in the *Tbx1*$^{-/-}$ OFT (Figure S1). Interestingly, the absence of *Tbx1* led to the upregulation of *Nppa* expression that was previously shown to be enriched in the sOFT.[12] Together, these results confirmed that *Pparγ* is preferentially enriched in a *Tbx1*-dependent region of the iOFT.

Inhibition of PPARγ Activity Impairs OFT Morphogenesis

To address the role of *Pparγ* in the regulation of the genetic signature of the OFT domains, inferior and superior OFT explant culture experiments were performed in the presence or absence of pharmacological modulators of PPARγ activity. OFTs were microdissected from E10.5 embryos and maintained in culture on collagen-coated dishes. Modulation of PPARγ signaling was examined in the presence of the PPARγ antagonist GW9662 or PPARγ ligand Rosiglitazone while control explants were cultured with vehicle solution (dimethyl sulfoxide [DMSO]). After 24 hours of treatment, the explants were processed for RT-qPCR to investigate the expression of PPARγ target genes identified in the IPA analysis. Inhibiting PPARγ activity with GW9662 in the iOFT explants leads to the downregulation of *Cd36* and upregulation of *Nppa* (Figure 2A). In contrast, PPARγ activation with Rosiglitazone in the sOFT displayed *Cd36* upregulation and *Nppa* downregulation (Figure 2A). Additional identified iOFT markers *Nrp2, Barx1,* and *Sema3c* also exhibited decreased expression upon PPARγ inhibition in the iOFT (Figure 2B), suggesting that PPARγ signaling is a major regulator of regionalized gene expression in the OFT.

To further study the role of PPARγ in the OFT morphogenesis, we performed rolling bottle culture of E8.5 embryos for 24 hours in the presence of the PPARγ antagonist GW9662. Pharmacological treatment did not affect the global development of the embryos. However, GW9662-treated embryos displayed impaired OFT morphogenesis (Figure 2C and 2D). Measurements of OFT length revealed that inhibition of PPARγ activity leads to a significantly shorter OFT compared to embryos exposed to vehicle (Figure 2E). This result suggests a role for PPARγ in the process of heart tube elongation from SHF progenitors, consistent with *Pparγ* expression in the distal OFT and transition zone. We next evaluated whether pharmacological modulation of PPARγ activity in embryo culture impacts the addition of the *Hoxb1* genetic lineage to the inferior wall of the OFT.[11] Our results using *Hoxb1*^{IRESCre};*Rosa26-YFP*$^{fl/fl}$ embryos revealed that GW9662-treated embryos display a reduced number of *Hoxb1* lineage labeled cells in the iOFT wall compared to vehicle-exposed embryos (Figure 2F and 2G). Consistent with these observations, whole-mount in situ hybridization revealed reduced transcript accumulation of the iOFT enriched gene *Sema3c* in the SHF and OFT of GW9662-treated embryos (Figure 2H and 2I). Together, these results indicate that PPARγ activity is required for the normal addition of SHF cells to the iOFT.

Mesodermal *Pparγ* Is Required for Normal Heart Development

To address the in vivo role of PPARγ in early cardiac progenitor cell deployment, conditional ablation of *Pparγ* was achieved using the *Mesp1-Cre* (early deletion in cranial and cardiac mesoderm) and *Mef2C-AHF-Cre* (deletion in SHF mesoderm) transgenic mouse lines. Using RT-qPCR experiments, we first validated that *Pparγ* is efficiently deleted in SHF from E9.5 *Mesp1-Cre;Pparγ*$^{fl/fl}$ (Figure S2A) and demonstrated no compensatory changes in expression of other PPAR family genes including *Pparα*

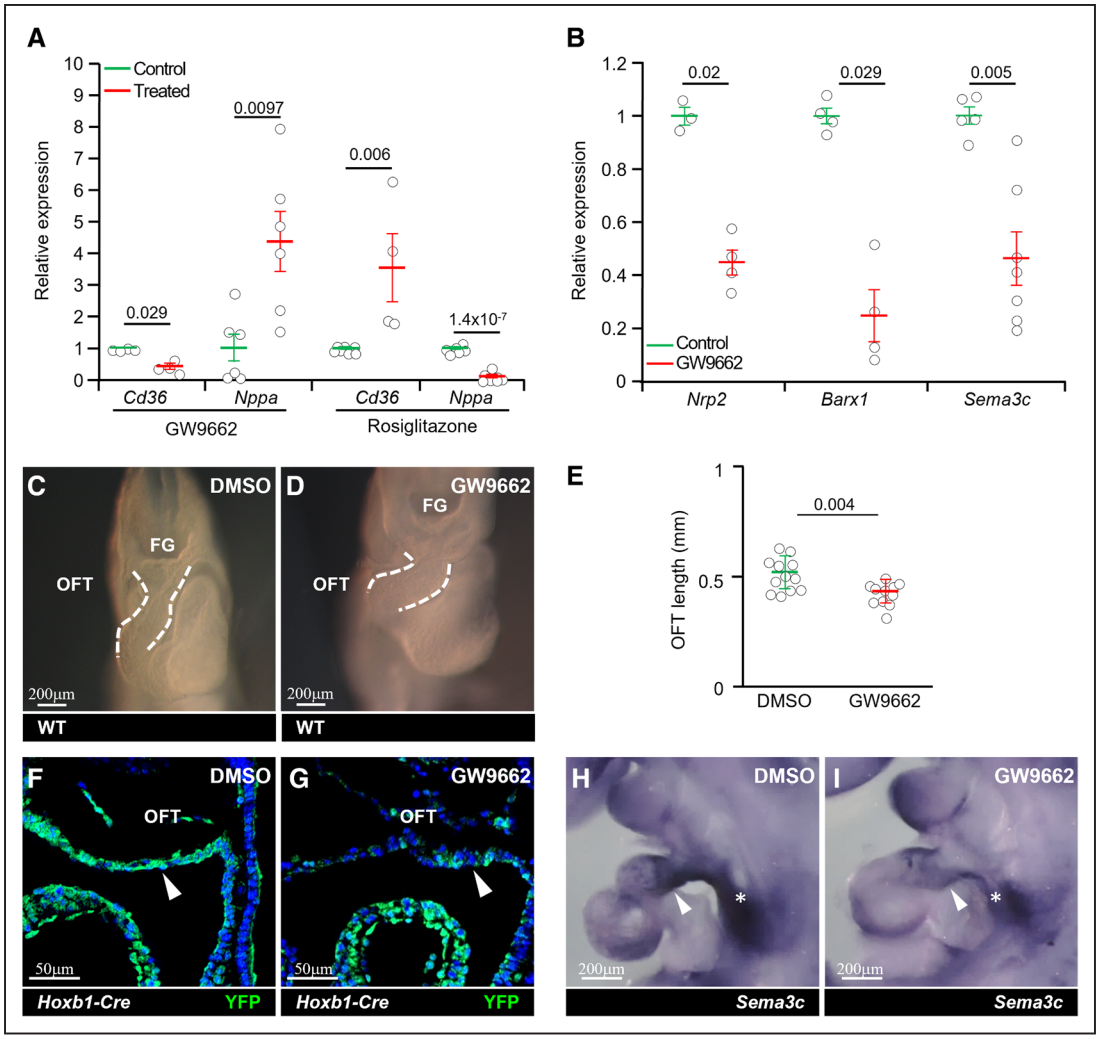

Figure 2. PPARγ (peroxisome proliferator-activated receptor gamma) regulates the genetic signature and morphogenesis of the outflow tract (OFT).

A, Quantitative reverse transcription polymerase chain reaction (qRT-PCR) results obtained from inferior and superior OFT (outflow tract) explants treated with GW9662 and Rosiglitazone, respectively. *Nppa* and *Cd36*, targets of *Pparγ*, are differentially regulated depending on the presence of PPARγ antagonist GW9662 or PPARγ synthetic ligand Rosiglitazone. Results are relative to vehicle-treated regions (N=4–7 per group and condition). **B**, qRT-PCR analysis of inferior wall of the OFT (iOFT) enriched genes, *Nrp2*, *Barx1,* and *Sema3c*, upon PPARγ inhibition with GW9662 in treated iOFT explant culture. Note that PPARγ signaling impairment affects the genetic signature of the OFT (N=3–7 per group). **C-E**, Embryonic day (E) 8.5 embryos were cultured for 24 hrs in the presence of GW9662 or DMSO (control). **C** and **D**, Ventral views of treated hearts. OFT elongation is impaired in GW9662-treated embryos. **E**, Measurement of the OFT length obtained from control (N=12) and GW9662-treated (N=11) embryos. **F** and **G**, Immunofluorescence on sagittal sections of *Hoxb1-Cre;RYFP* embryos, showing reduced YFP (yellow fluorescent protein) labeled cells (arrowheads) in the iOFT of GW9662-treated embryo compare to control (N=5–6 per condition). **H** and **I,** Left views of whole-mount in situ hybridization showing decreased *Sema3c* expression in the OFT (arrowhead) and the Second Heart Field (asterisks) after GW9662-treatment (arrowheads, N=3 per condition). FG, foregut; OFT, outflow tract. Presented results are representative of biological replicates. Statistics: 2-tailed *t* test (**A**, **E**), Mann-Whitney *U* test (**A** and **B**), and Kolmogorov-Smirnov test (**B**); please see the Major Resources Table in the Supplemental Material. DMSO indicates dimethyl sulfoxide; FG, foregut; and WT, wild-type.

and *Pparδ* (Figure S2A). Analysis of E10.5 and E15.5 *Mesp1-Cre;Pparγ*$^{fl/fl}$ mutant embryos showed no significant embryonic lethality. However, morphological and histological examinations of *Mesp1-Cre;Pparγ*$^{fl/fl}$ embryos revealed anomalies in heart development. At E10.5, a significant shortening of the OFT was observed in *Mesp1-Cre;Pparγ*$^{fl/fl}$ mutant hearts (N=11) compared to control littermates (N=8; Figure 3A through 3C). The observed decrease in OFT length suggests a defect in SHF deployment. We therefore evaluated SHF proliferation in E9.5 control and conditional mutant embryos by scoring the number of cells positive for the mitotic marker PH3 (phospho-histone 3). Our results revealed that *Isl1*$^{+}$ and MF20 (myosin heavy chain antibody)$^{-}$ SHF cells in the dorsal pericardial wall and pharyngeal mesenchyme displayed a significant reduction in proliferative activity in conditional mutant (N=5) compared to control embryos (N=4; Figure 3D through 3F). In situ hybridization analysis of conditional mutant embryos revealed a substantial reduction of *Sema3c* transcript accumulation in the SHF

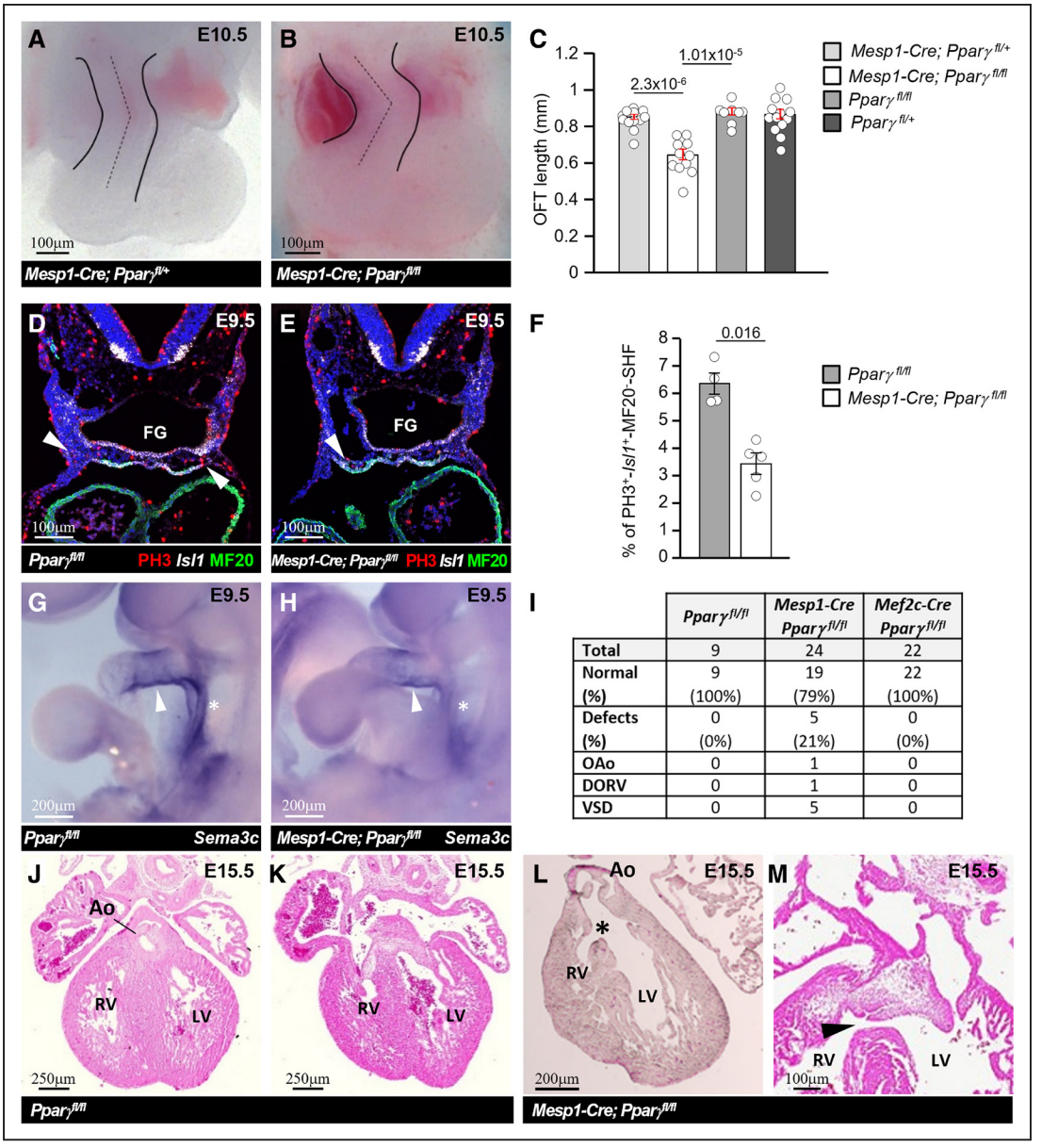

	Pparγ fl/fl	Mesp1-Cre Pparγ fl/fl	Mef2c-Cre Pparγ fl/fl
Total	9	24	22
Normal (%)	9 (100%)	19 (79%)	22 (100%)
Defects (%)	0 (0%)	5 (21%)	0 (0%)
OAo	0	1	0
DORV	0	1	0
VSD	0	5	0

Figure 3. Cardiac development defects in conditional *Pparγ* mutant embryos.
A and **B,** Ventral views of embryonic day (E) 10.5 *Mesp1-Cre;Pparγ*$^{fl/fl}$ and *Mesp1-Cre;Pparγ*$^{fl/+}$ hearts. Outflow tract (OFT) elongation is affected in *Mesp1-Cre;Pparγ*$^{fl/fl}$ hearts. **C**, Measurement of the OFT length showing that E10.5 *Mesp1-Cre;Pparγ*$^{fl/fl}$ OFT is significantly shorter (N=8–13 per genotype). **D** and **E**, Immunofluorescence on transverse sections showing PH3 (phospho-Histone 3), *Isl1*, and MF20 staining. **F**, PH3 quantification in *Isl1*$^{+}$-MF20^{-} cells reveals decreased Second Heart Field (SHF) proliferation in *Mesp1-Cre;Pparγ*$^{fl/fl}$ (N=5) compared to control (N=4) E9.5 embryos. **G** and **H**, Left views of whole-mount in situ hybridization showing reduced *Sema3c* expression in the inferior wall of the OFT (iOFT; arrowhead) and the SHF (asterisks) of E9.5 *Mesp1-Cre;Pparγ*$^{fl/fl}$ embryo (N=3–4 per genotype). **I**, Cardiac defects scored after analysis of histological sections at E15.5 in *Mesp1-Cre;Pparγ*$^{fl/fl}$ and *Mef2c-Cre;Pparγ*$^{fl/fl}$ conditional mutants and *Pparγ*$^{fl/fl}$ control littermates. **J–M**, Eosin-stained sections of E15.5 hearts revealing that conditional *Mesp1-Cre;Pparγ*$^{fl/fl}$ mutants display congenital heart defects including an overriding aorta (asterisk) and a membraneous ventricular septal defect (arrowhead). Presented results are representative of biological replicates. Statistics: 2-tailed *t* test (**C**) and Mann-Whitney *U* test (**F**); please see the Major Resources Table in the Supplemental Material. Ao indicates aorta; DORV, double outlet right ventricle; FG, foregut; LV, left ventricle; MF20, Myosin Heavy Chain Antibody (MF20); OAo, overriding aorta; RV, right ventricle; and VSD, ventricular septal defect.

and OFT (Figure 3G and 3H), consistent with our *ex vivo* results (Figure 2I). Histological analysis of E15.5 *Mesp1-Cre;Pparγ*$^{fl/fl}$ hearts revealed conotruncal CHD in 21% of the *Mesp1-Cre;Pparγ* $^{fl/fl}$ hearts including overriding aorta (1/24), double outlet right ventricle (1/24) and ventricular septal defects (5/24) while no defects were observed in *Pparγ* $^{fl/fl}$ control littermates (0/9; $P<0.05$; Figure 3I through 3M). We further investigated the role of *Pparγ* in OFT development using the *Mef2c-AHF-Cre* (*Mef2c-Cre*) line in which Cre is expressed in the SHF. Surprisingly, while efficient *Pparγ* deletion is observed in SHF from E9.5 *Mef2C-AHF-Cre;Pparγ*$^{fl/fl}$ (Figure S2B)

no defects in cardiac morphogenesis were observed in *Mef2C-AHF-Cre;Pparγ*$^{fl/fl}$ mutant hearts at E10.5 or E15.5 (Figure 3I). Thus, our results suggest that *Pparγ* is required for arterial pole development in early cardiac progenitor cells before expression of *Mef2c-AHF-Cre*.

Hes1 Controls *Pparγ* Expression in the Superior Part of the OFT

We previously demonstrated that the *A17-Myf5-nlacZ-T55* transgene, which expresses a β-galactosidase reporter gene in future subaortic myocardium in the early mouse embryo, has integrated upstream of *Hes1* on chromosome 16.[9,10,14] *Hes1* encodes a transcriptional repressor[37] and has been shown to play an important role in arterial pole development.[14,38] In other cellular contexts HES1 has been shown to directly repress *Pparγ* expression.[39,40] We thus hypothesized that HES1 represses *Pparγ*, allowing enrichment of genes negatively regulated by PPARγ in the sOFT.

To precisely compare the *Hes1*-dependent *A17-Myf5-nlacZ-T55* transgene (*Hes1-Tg*) expression domain with that of *Pparγ* at early embryonic stages, we analyzed β-galactosidase and *Pparγ* expression together with SHF marker and genetic lineage analysis. Between E8.5 and E9.5, β-galactosidase expression is observed in a subpopulation of *Isl1*-expressing SHF progenitor cells in the anterior region of the dorsal pericardial wall, contiguous with sOFT myocardium (Figure 4A and 4D). In situ hybridization experiments for *Wnt11* and *Sema3c*, markers of the superior and inferior OFT walls, respectively,[9,20] revealed that expression of the *Hes1*-transgene and *Wnt11* overlap in the anterior SHF and sOFT (Figure S3A through S3C). This confirms expression of the *Hes1*-transgene in the sOFT but not iOFT, where *Pparγ* and *Tbx1* are enriched (Figure 4E and I4).

Hoxb1-expressing SHF progenitors, located in the posterior SHF, contribute to the iOFT and subsequently to subpulmonary myocardium.[12] Genetic lineage tracing experiments using *Hoxb1*^{IRESCre};*Rosa26-YFP*$^{fl/fl}$;*Hes1*-transgene embryos demonstrate that the *Hes1*-dependent *A17-Myf5-nlacZ-T55* transgene expression in the sOFT does not overlap with the *Hoxb1* genetic lineage in the iOFT (Figure 4B and 4C), indicating that *Hes1*-expressing subaortic myocardial progenitors are not derived from *Hoxb1*-expressing progenitor cells. *Hoxb1*-derived OFT myocardium is known to be *Tbx1*-dependent.[12] Fluorescent *in situ* hybridization performed at E8.5 and E9.5 established that *Hes1*-expressing cells are localized in the sOFT, in contrast to *Tbx1* or *Pparγ* expressing cells in the iOFT (Figure S3D through S3F). These results confirm that the *Hes1*-expressing domain defines a *Wnt11* positive subpopulation of SHF cells that is independent of the *Hoxb1*-lineage and *Tbx1* negative.

To determine whether HES1 controls *Pparγ* expression in the OFT, RT-qPCR analyses were performed on isolated OFTs from E10.5 wild-type and *Hes1*$^{-/-}$ mutant embryos. *Pparγ* levels were significantly increased in the absence of *Hes1* (Figure 4F). In addition, the PPARγ target genes *ApoE* and *Cd36*, which are normally expressed in the iOFT,[12] are significantly upregulated in *Hes1*$^{-/-}$ mutant OFTs (Figure 4F). In situ hybridization experiments performed on E10.5 *Hes1*-mutant embryos support this result by showing the expansion of *Pparγ* expression in the sOFT of *Hes1*$^{-/-}$ compared to wild-type embryos (Figure 4G and 4H). Moreover, immunofluorescence experiments performed at E9.5 on wild-type and *Hes1*$^{-/-}$ mutant embryos demonstrate that the absence of *Hes1* leads to the accumulation of PPARγ in the sOFT (Figure 4I and 4J), as well as expression in the iOFT. Taken together, these results suggest that *Hes1* regulates the transcriptional identity of the OFT subdomains by repressing *Pparγ* expression.

Hes1 Is Required for the Development of the Arterial Pole of the Heart

We initially identified *Hes1* as a regulator of arterial pole development.[14] Indeed, *Hes1*$^{-/-}$ embryos display defects in OFT elongation and alignment resulting in conotruncal defects. However, *Hes1* conditional deletion in cardiac neural crest cells or in pharyngeal ectoderm does not impair elongation of the OFT.[38] This suggests that specific expression of *Hes1* in the SHF may contribute to OFT morphogenesis. To evaluate the specific requirement of *Hes1* in SHF progenitors, we conditionally ablated *Hes1* using *Mesp1-Cre* and *Mef2c-AHF-Cre*. *Mesp1-Cre;Hes1*$^{+/-}$ and *Mef2c-AHF-Cre;Hes1*$^{+/-}$ mice were crossed with *Hes1*$^{fl/fl}$ mice and OFT morphogenesis and cardiac defects were assessed (Figure 5). Two out of 22 analyzed E15.5-E16.5 *Mesp1-Cre;Hes1*$^{-/fl}$ hearts (9% penetrance) displayed conotruncal defects including overriding aorta, double outlet right ventricle and ventricular septal defects (Figure 5A through 5J). Analysis of E10.5 *Mesp1-Cre*;*Hes1*$^{-/fl}$ compared to control *Hes1*$^{+/fl}$ embryos revealed that the OFT was significantly shorter and straighter than in control embryos (Figure 5K through 5N). Elevated numbers of normal *Mesp1-Cre;Hes1*$^{-/fl}$ hearts were obtained at fetal stages suggesting thus a degree of phenotypic recovery. The analysis, in E9.5 embryos, of SHF progenitor (*Isl1*$^{+}$ and MF20^{-}) cell proliferation, by scoring the mitotic marker PH3 (Figure 5O and 5P), revealed significantly reduced SHF proliferative activity in *Mesp1-Cre*;*Hes1*$^{-/fl}$ compared to control *Hes1*$^{+/fl}$ embryos (Figure 5Q). Despite efficient *Hes1* deletion in the E9.5 *Mef2c-AHF-Cre*;*Hes1*$^{-/fl}$ SHF (Figure S4), no cardiac defects were observed in hearts obtained from the *Mef2c-AHF-Cre*;*Hes1*$^{-/fl}$ embryos (N=19; Figure 5J). Together with our observations on *Pparγ* conditional mutant embryos, these data suggest that early roles of *Hes1* and *Pparγ* during SHF development are required for subsequent OFT development.

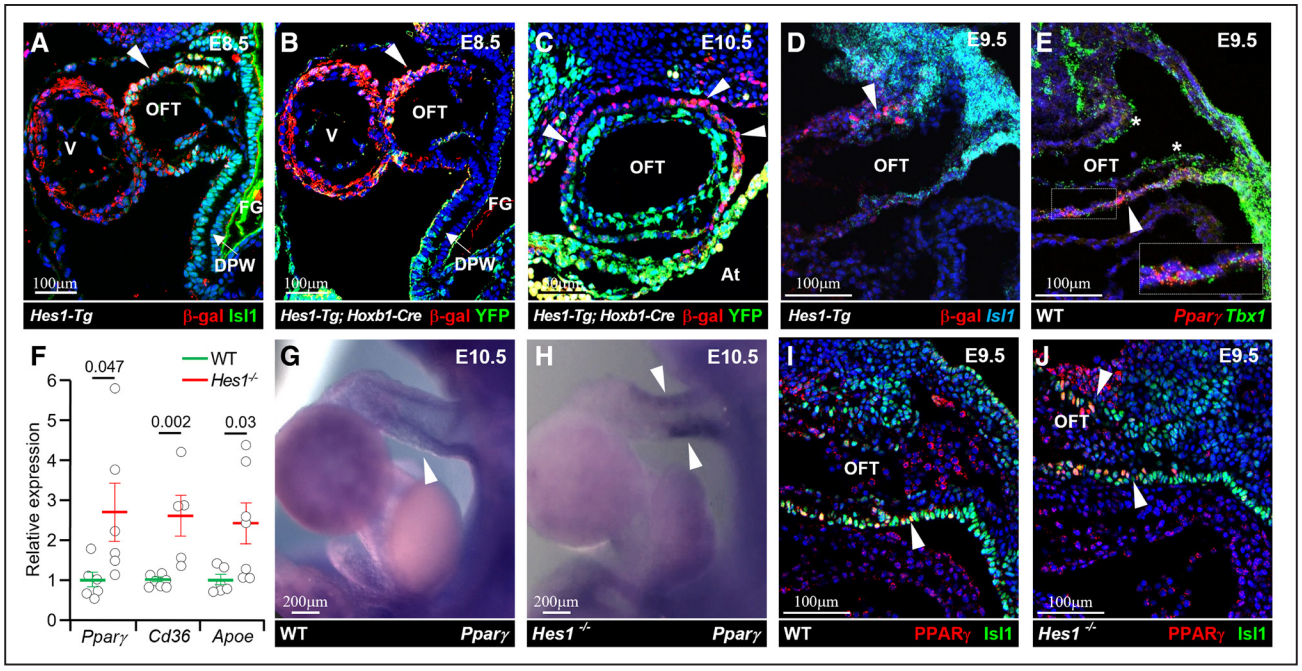

Figure 4. Hes1 negatively regulates Pparγ (peroxisome proliferator–activated receptor gamma) outflow tract (OFT) expression. **A**, Immunofluorescence on sagittal section of a embryonic day (E) 8.5 *Hes1-Tg* embryo showing that Isl1 (ISLET LIM homeobox 1) is expressed in Second Heart Field (SHF) progenitors. *Hes1-Tg* cells are restricted to the superior wall of the OFT (sOFT; β-gal [β-galactosidase]; arrowhead; N=5). **B** and **C**, Immunofluorescence of *Hes1-Tg;Hoxb1-Cre;*RYFP) embryos showing the absence of overlap between *Hes1-Tg* cells (β-gal) and the *Hoxb1* lineage (YFP) in the OFT. **B**, Sagittal section of E8.5 embryo showing *Hes1-Tg* cells in the sOFT (arrowheads) and YFP cells in the posterior DPW (arrow, N=3). **C**, Truncal section of the OFT at E10.5 showing *Hes1-Tg* cells in the sOFT (arrowheads) and the YFP cells in the inferior wall of the OFT (iOFT; N=3). **D**, RNAscope combined with immunofluorescence on sagittal sections of *Hes1-Tg* at E9.5 (N=3). *Hes1-Tg* cells (arrowhead) accumulate in Isl1-expressing SHF progenitors in the sOFT. **E**, RNAscope with *Pparγ* and *Tbx1* riboprobes showing enrichment of both transcripts in the iOFT (arrowhead). Inset, high magnification of the iOFT (N=5). **F**, Quantitative reverse transcription polymerase chain reaction analysis of *Pparγ*, *Cd36*, and *ApoE* transcript levels in E10.5 *Hes1*$^{-/-}$ OFT relative to wild-type (WT; N=5–7 per conditions). **G** and **H**, Left views of E10.5 embryos after in situ hybridization with *Pparγ* riboprobe. **G**, Wild-type (WT) embryo with localized enrichment of *Pparγ* expression in the iOFT (arrowhead, N=4). **H**, *Hes1*$^{-/-}$ embryo displaying an increase in *Pparγ* expression level in both the superior and inferior OFT (arrowheads, N=3). **I** and **J**, Immunofluorescence on sagittal sections of E9.5 embryos. **I**, WT embryo displaying localized enrichment of PPARγ in the iOFT (arrowhead; N=3). **J**, *Hes1*$^{-/-}$ embryo displaying PPARγ in both sOFT and iOFT (arrowheads; N=3). Presented results are representative of biological replicates. Statistics: 2-tailed *t* test (**F**) and Mann-Whitney *U* test (**F**); please see the Major Resources Table in the Supplemental Material. DPW indicates dorsal pericardial wall; FG, foregut; *Hes1-Tg, A17-Myf5-nlacZ-T55* transgene; OFT, outflow tract; and V, ventricle.

NOTCH/HES1 Signaling Regulates *Pparγ* Expression in the OFT

Since *Hes1* is a downstream target of the NOTCH signaling pathway[37] we addressed the role of the NOTCH/HES1 pathway in the regulation of *Pparγ* expression in SHF progenitors and OFT wall. Activation of NOTCH receptors leads to a γ-secretase mediated proteolytic cleavage and release of the NICD1 (NOTCH intracellular domain) which then translocates to the nucleus to transcriptionally activate downstream target genes, including *Hes1*.[41] Active NOTCH signals have already been described in the OFT, endocardium and arterial endothelial cells[42] and important roles for NOTCH signaling have also been identified in the SHF.[43,44] In addition, recent evidence demonstrated a requirement for NOTCH signaling in SHF progenitor cell proliferation.[45] Immunofluorescence experiments using an antibody detecting NICD1 revealed that active NOTCH signaling occurs preferentially in the sOFT wall coincident with the *Hes1*-transgene expressing domain (Figure 6A and 6B). Indeed, NICD1 is enriched in *Isl1* positive (Figure 6C), *Hoxb1*-lineage negative (Figure 6D), cells in the sOFT, confirming spatially restricted active NOTCH signaling in the future subaortic myocardial domain. Therefore, active NOTCH signaling in the superior part of the OFT may operate upstream of *Hes1* expression.

We then investigated the role of regionalized NOTCH signaling in the regulation of *Hes1* expression in the OFT. E8.5 embryos expressing the *Hes1*-transgene were cultured for 24 hrs in the presence of DAPT ((2S)-N-[(3,5-Difluorophenyl)acetyl]-L-alanyl-2-phenyl] glycine 1,1-dimethylethyl ester), a γ-secretase complex inhibitor. While DAPT treatment had no impact on global embryonic growth, NOTCH signaling inhibition results in reduced transgene expression as depicted by β-galactosidase staining (Figure 6E through 6H). Immunofluorescence analysis revealed a striking decrease in the number of β-galactosidase-expressing cells in the superior wall of the OFT myocardium (Figure 6I and 6J).

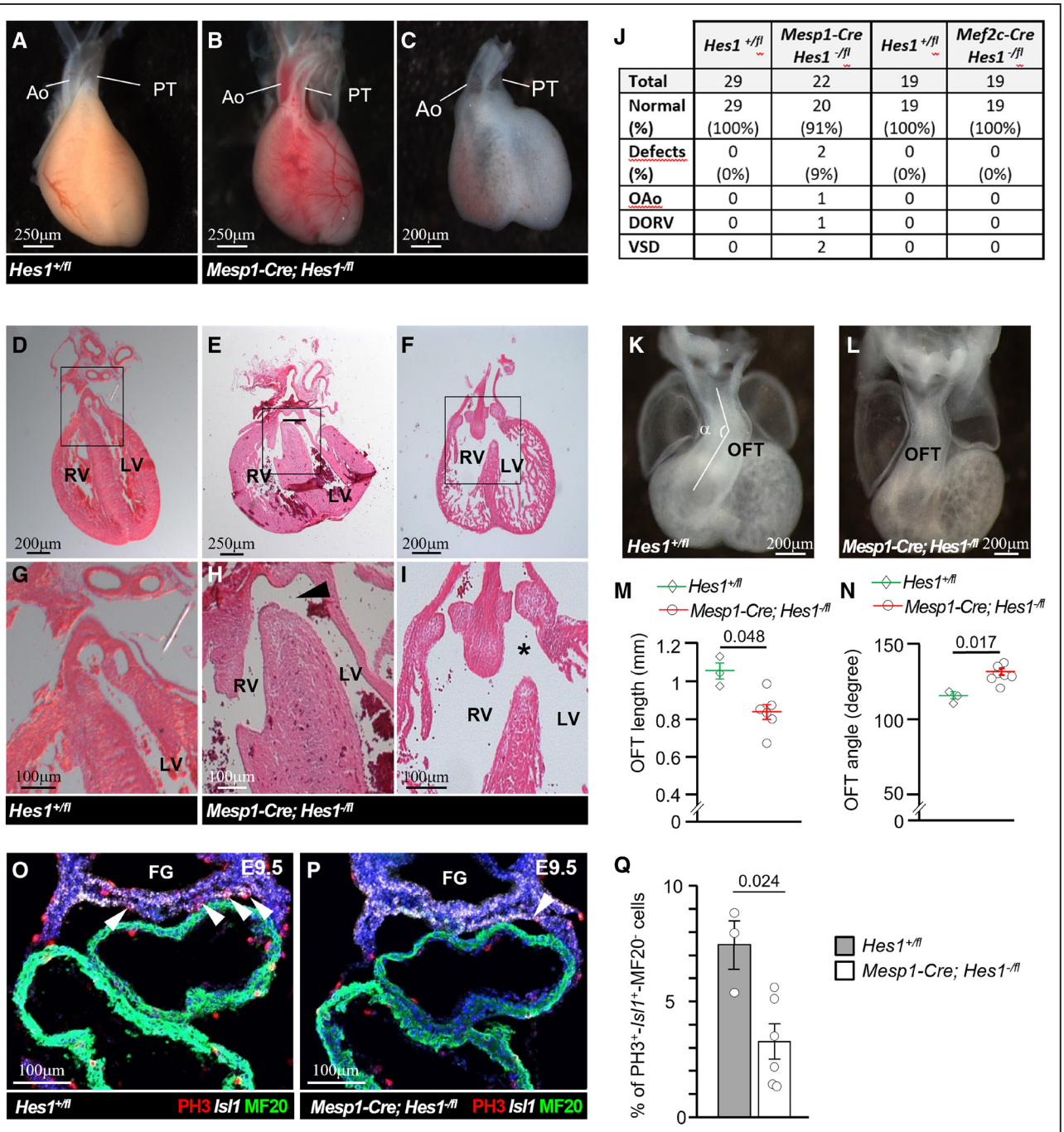

J	Hes1 +/fl	Mesp1-Cre Hes1 -/fl	Hes1 +/fl	Mef2c-Cre Hes1 -/fl
Total	29	22	19	19
Normal (%)	29 (100%)	20 (91%)	19 (100%)	19 (100%)
Defects (%)	0 (0%)	2 (9%)	0 (0%)	0 (0%)
OAo	0	1	0	0
DORV	0	1	0	0
VSD	0	2	0	0

Figure 5. Impaired outflow tract development in *Hes1* conditional mutant embryos.
A–**C,** Ventral views of embryonic day (E) 18.5 hearts and (**D**–**I**), eosin-stained sections showing that *Mesp1-Cre;Hes1*$^{-/Flox}$ mutants display congenital heart defects including ventricular septal defects (VSD; arrowhead), overriding aorta (arrowhead) and dextraposed aorta (asterisks) with double outlet right ventricle. Black squares identify the position of high magnification views shown in the bottom panels. **J,** Scoring of cardiac defects in E15.5–E18.5 conditional mutant and control littermate hearts analyzed by histological sections. **K** and **L,** Ventral views of E10.5 *Hes1*$^{+/fl}$ and *Mesp1-Cre;Hes1*$^{-/Flox}$ hearts. Outflow tract (OFT) length and angle landmarks used for OFT measurements are indicated. **M**, Histograms showing E10.5 *Hes1*$^{+/fl}$ (N=3) and *Mesp1-Cre;Hes1*$^{-/fl}$ (N=6) OFT length. **N**, Histograms showing E10.5 *Hes1*$^{+/fl}$ (N=3) and *Mesp1-Cre; Hes1*$^{-/fl}$ (N=7) OFT angle measurements. Mutant hearts display a shorter and straighter OFT. **O** and **P**, Immunofluorescence on transverse sections showing PH3 (phospho-Histone 3), *Isl1,* and MF20 (myosin heavy chain antibody) staining. **Q**, PH3 quantification in *Isl1*$^{+}$ MF20 cells reveals decreased Second Heart Field proliferation in *Mesp1-Cre;Hes1*$^{-/fl}$ (N=6) compared to control (N=3) E9.5 embryos. Presented results are representative of biological replicates. Statistics: Mann-Whitney *U* test; please see the Major Resources Table in the Supplemental Material. Ao indicates aorta; DORV, double outlet right ventricle; LV, left ventricle; OAo, overriding aorta; PT, pulmonary trunk; and RV, right ventricle.

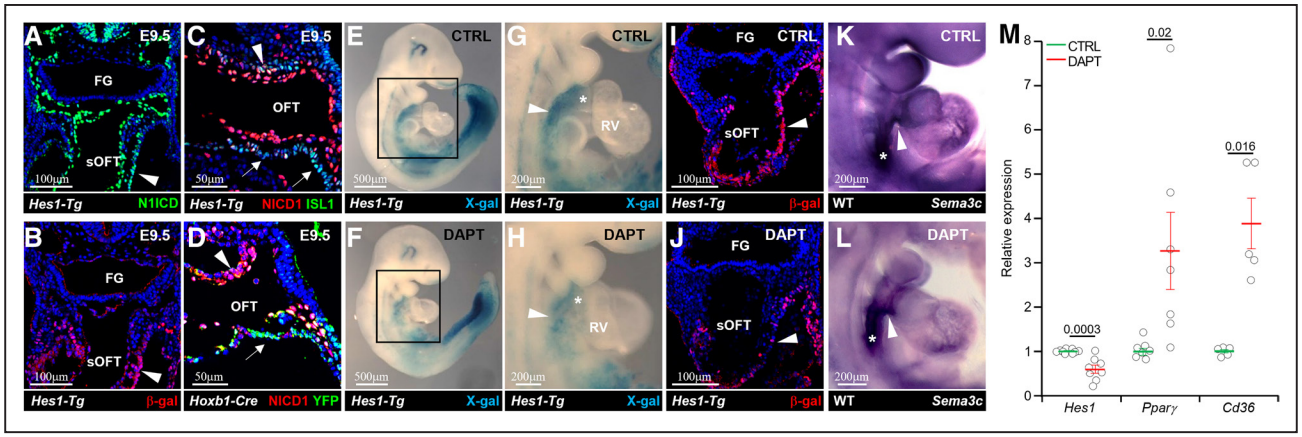

Figure 6. NOTCH (Notch receptor 1)/HES1 (Hes family bHLH transcription factor 1) signaling regulates regional expression domains in outflow tract (OFT) myocardium.

A–**D**, Embryonic day (E) 9.5 Transverse (A-B) and sagittal (C-D) sections at the level of the OFT (N=5). **A**–**B**, Immunofluorescence of serial sections of *Hes1-Tg* embryo showing identical pattern of NICD1 (Notch intracellular domain 1) and β-gal (β-galactosidase) expressions in the superior wall of the OFT (sOFT; arrowheads). Note NICD1 expression in the endothelial cells of the OFT, aortic sac, and great arteries. **C**, Immunofluorescence of *Hes1-Tg* embryo showing identical pattern of expression of NICD1 and ISL1 (ISLET LIM homeobox 1) in the sOFT (arrowhead). ISL1 is also observed in the inferior wall of the OFT (iOFT) and DPW (arrows). NICD1 is also detected in the endothelial cells. **D**, Immunofluorescence of *Hoxb1-Cre;RYFP* embryo showing the absence of overlap between NICD1 in the sOFT (arrowhead) and YFP cells in the iOFT (arrow). Double positive NCID1, YFP cells are endothelial. **E–J**, Results obtained from *Hes1-Tg* embryos maintained in culture from E8.5 to E9.5 with DMSO (control [CTRL]; **E**, **G**, **I**) or DAPT ((2S)-N-[(3,5-Difluorophenyl)acetyl]-L-alanyl-2-phenyl]glycine 1,1-dimethylethyl ester; **F**, **H**, **J**). **E**–**H**, Right views of X-gal–stained embryos. In control embryo, a large number of cells are located behind the heart where a reduced number of *Hes1-Tg* cells is detected in DAPT-treated embryo (arrowheads). The OFT length is shorter in DAPT-treated (N=6) compared to control (asterisks, N=9) embryos. **G** and **H**, High magnifications. **I** and **J**, Immunofluorescence on transverse sections at the level of sOFT showing less *Hes1-Tg* cells in DAPT-treated (N=3) compared to control (arrowheads, N=5) embryo. **K** and **L,** Right views of embryos after *Sema3c* (semaphorin 3C) in situ hybridization showing no change in transcript enrichment neither in the pharyngeal region (asterisks) nor in the iOFT (arrowheads) after DAPT treatment (N=3 per condition). The OFT is shorter in DAPT-treated embryos. **M**, Quantitative reverse transcription polymerase chain reaction analysis of *Hes1*, *Pparγ*, and *Cd36* transcript levels in the OFT from DAPT-treated embryos relative to OFT from CTRL-treated embryos (N=5–9 per group and condition). Presented results are representative of biological replicates. Statistics: 2-tailed *t* test (**M**) and Mann-Whitney *U* test (**M**); please see the Major Resources Table in the Supplemental Material. FG indicates foregut; *Hes1-Tg, A17-Myf5-nlacZ-T55* transgene; RV, right ventricle; WT, wild-type; and X-gal, β-galactosidase labelling.

In contrast, the complementary OFT domain, characterized by *Sema3c* expression, was unaffected (Figure 6K and 6L). These results suggest that *Hes1*-transgene expression in future subaortic myocardial cells is regulated by Notch signaling.

To investigate NOTCH/HES1 control of *Pparγ* OFT expression, OFT explant cultures were treated with DAPT (Figure 6M). RT-qPCR measurements obtained from DAPT-treated OFT explants identified a decrease in *Hes1* expression and an increase in expression of *Pparγ* and the PPARγ direct downstream target *Cd36*. Thus, NOTCH signaling inhibition leads to changes in the expression of OFT regionalized genes suggesting that NOTCH/HES1 signaling may determine the sOFT transcriptional identity by controlling *Pparγ* expression.

Delta-Like 1 Regulates Notch/Hes1-Dependent Repression of *Pparγ*

DLK1 (PREF1 [preadipocyte factor 1]) is a noncanonical NOTCH ligand, known to be involved in the repression of *Pparγ* expression.[46] We investigated whether DLK1 may contribute to the control of regional transcriptional identity in the OFT. Using in situ hybridization we found that DLK1 is regionally expressed in the OFT at early developmental stages. At E8.5, *Dlk1* expression is observed in cells at the cranial side of the arterial pole and in cells in the pharyngeal region (Figure 7A) close to the arterial pole that also expresses the *Hes1*-transgene and *Wnt11* (Figure S3). At E9.5 and E10.5, *Dlk1* expression is observed in the sOFT, but not iOFT (Figure 7B and 7C), thus showing a strikingly complementary expression pattern to that of *Pparγ* (Figure 1). Consistently and similarly to the *Hes1*-transgene expression domain, at E12.5 *Dlk1* is expressed in myocardium at the base of the aorta (Figure 7D and 7E). In addition, the *Dlk1* expression domain is expanded in *Tbx1*$^{-/-}$ hearts except for a small negative myocardial domain on the left side of the common trunk (Figure 7F). This is consistent with expression of the *Hes1*-transgene in *Tbx1* null hearts and highlights the *Tbx1*-dependence of iOFT and subpulmonary myocardium development.[9] Thus, colocalization of *Dlk1* with NICD1 and the *Hes1*-transgene in the sOFT suggests that activation of NOTCH signaling in these cells may be autocrine, consistent with previously documented autocrine NOTCH signaling in the SHF.[43]

As shown above, *Hes1* negatively regulates *Pparγ* expression in the sOFT downstream of NOTCH signaling.

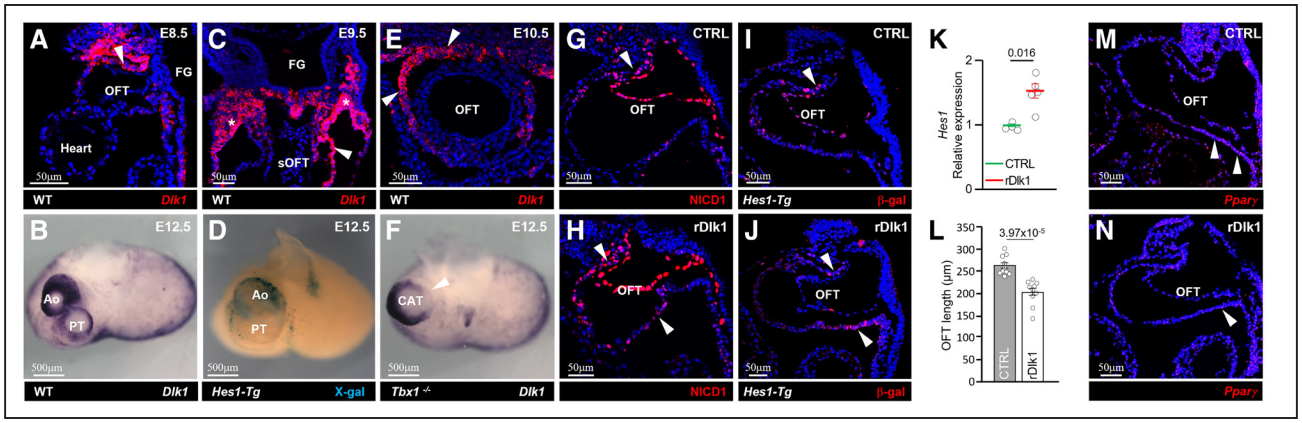

Figure 7. Delta-like noncanonical Notch ligand 1 (*Dlk1*) is expressed in the superior wall of the OFT (sOFT) and subaortic myocardium.

A–**C**, In situ hybridization showing *Dlk1* expression in the Second Heart Field and sOFT (arrowheads, N=5 per stage). **A**, Sagittal section at embryonic day (E) 8.5 showing *Dlk1* expression in the sOFT (arrowhead) close to the arterial pole. **B**, E9.5 Transverse section showing *Dlk1* expression in the sOFT (arrowhead) and pharyngeal mesoderm (asterisks). **C**, E10.5 truncal section showing *Dlk1* expression in the sOFT (arrowheads). **D**–**F**, Superior views of E12.5 hearts. **D**, In situ hybridization of wild-type (WT) heart with localized enrichment of *Dlk1* at the base of the aorta (N=3). **E**, Superior view of a X-gal (β-galactosidase labelling)-stained *Hes1-Tg* heart showing *LacZ*-expressing cells at the base of the aorta (N=3). **F**, In situ hybridization showing enrichment of *Dlk1* around the common arterial trunk (CAT) of a *Tbx1*$^{-/-}$ heart with a negative region at the right dorsal location (arrowhead, N=3). **G**–**H**, Immunofluorescence of sagittal sections of E9.5 control (CTRL) and rDlk1 (recombinant DLK1)-treated embryos showing an increase in NICD1 (Notch intracellular domain 1) in the sOFT and inferior wall of the OFT (iOFT; arrowheads) of rDlk1-treated embryo (N=3–5 per condition). **I** and **J**, Immunofluorescence on sagittal sections from CTRL and rDlk1-treated *Hes1-Tg* embryos showing increased *Hes1-Tg* cell numbers in the iOFT of rDlk1-treated (arrowheads, N=5) compared to control (N=8) embryos. **K**, Quantitative reverse transcription polymerase chain reaction for *Hes1* transcripts in rDlk1-treated iOFT explants relative to control showing a significant increase in transcript level upon rDlk1 treatment (N=4–5 per condition). **L**, Histogram showing that, compared to controls (N=10), rDlk1-treated embryos display a shorter distal OFT (N=10). **M** and **N**, Fluorescent in situ hybridization on sagittal sections at the level of the OFT on CTRL (N=3) and rDLK1-treated E9.5 embryos (N=3) showing reduced *Pparγ* expression in the rDLK1-treated iOFT. Presented results are representative of biological replicates. Statistics: 2-tailed *t* test (**L**) and Mann-Whitney *U* test (**K**); please see the Major Resources Table in the Supplemental Material. Ao indicates aorta; FG, foregut; *Hes1-Tg, A17-Myf5-nlacZ-T55* transgene; and PT, pulmonary trunk.

Indeed, increased *Pparγ* expression was observed in *Hes1*$^{-/-}$ (Figure 4F through 4J) and DAPT-treated OFTs (Figure 6M). Given these results and that *Dlk1* encodes a noncanonical ligand for NOTCH receptors and given that *Dlk1* is strictly expressed in the cells with active NOTCH signaling, we hypothesized that DLK1 may be an upstream activator of NOTCH/HES1 signaling in the sOFT. To address this point, E8.5 embryos were cultured in rolling bottles for 24 hours in the presence of recombinant DLK1 protein and the impact on NOTCH signaling activation was monitored using NICD1 immunofluorescence experiments (Figure 7G and 7H). Compared to controls, DLK1-treated embryos display a significant increase in NICD1 signals. NICD1 positive cells were observed in the sOFT and iOFT after exposure to recombinant DLK1 (Figure 7H), consistent with ectopic activation of NOTCH signaling in the iOFT by DLK1. RT-qPCR and immunofluorescence experiments revealed that treatment with recombinant DLK1 protein for 24 hours also led to an increase in *Hes1* transcript levels in iOFT explants and activation of the *Hes1* enhancer trap transgene in the iOFT wall (Figure 7I through 7K). To investigate the impact of regional DLK1/NOTCH/HES1 signaling alteration on OFT morphogenesis, OFT length measurements were performed and revealed that treatment with recombinant DLK1 leads to a significantly shorter OFT compared to embryos exposed to vehicle (Figure 7L and Figure S5). Finally, the evaluation of *Pparγ* expression using fluorescent in situ hybridization demonstrated that upregulated DLK1/NOTCH/HES1 signaling in the iOFT results in reduced *Pparγ* expression (Figure 7M and 7N). Together, these results demonstrate that DLK1 participates in the activation of regional NOTCH/HES1 signaling that may be critical for PPARγ pathway regulation in the developing OFT.

DISCUSSION

Here we provide new insights into the regulatory pathways operating in subdomains of the developing cardiac OFT. In particular, we show that *Pparγ* is expressed in *Tbx1*-dependent future subpulmonary myocardial cells in the inferior wall of the OFT and is required in early cardiac mesoderm for normal outflow tract development. *Pparγ* expression is repressed by NOTCH/HES1 signaling in the superior wall of the OFT. We identify the noncanonical NOTCH ligand DLK1 as a potential upstream NOTCH/HES1 signaling regulator in the sOFT wall.

Our findings extend previous results establishing that the inferior and superior walls of the OFT display distinct genetic signatures and are added at different developmental stages from the SHF.[12] Using IPA bioinformatic

analysis, we first identified specific enrichment of PPAR signaling pathway related genes in the inferior OFT. This is consistent with earlier identification of *Pparγ* being among the top 5 transcripts enriched in the inferior versus superior OFT. Further analysis identified regionalized enrichment of potential positive and negative PPARγ targets in the inferior and superior OFT, respectively, including *Cd36*, involved in fatty acid cell transport,[47] *G0S2,* required in terminal adipogenic process[48] and the PPARγ cofactor, PPARGC1A, a transcriptional target of *Pparγ*.[48–50] The regional transcriptional control of this PPARγ related-gene network in the OFT is the result of dual regulation of *Pparγ* expression by TBX1 and HES1, regulators of complementary populations of arterial pole progenitor cells in the SHF.[9,14] *Pparγ* is expressed in a *Tbx1*-dependent domain of the OFT. This may result from direct transcriptional activation of *Pparγ* by TBX1 in the iOFT and/or inhibition by HES1 in the sOFT. In support of direct regulation by TBX1, reduced *Pparγ* expression has been observed in *Tbx1* siRNA knockdown mouse stromal vascular cells.[51] Moreover, T-box binding elements are present at the *Pparγ* locus[52] and reduced *Pparγ* transcript levels are observed in the *Tbx1*$^{+/-}$ OFT (data not shown). *Pparγ* inhibition by HES1 most likely occurs through direct transcriptional regulation due to evidence for HES1 binding to target regulatory elements in the *Pparγ* promoter.[39,40] Studies have also shown that HES1 can directly repress the gene encoding the transcriptional coactivator of PPARγ, *Ppargc1a*.[53] Consistent with our observations, the *Ppargc1a* locus was recently shown to be bound and potentially regulated by TBX1[54] suggesting that *Ppargc1a* acts together with *Pparγ* in regulating regional transcription in the OFT. Together these observations implicate PPARγ as a component of cross-regulatory transcriptional programs operating in distinct OFT subdomains.

Cardiomyocyte-specific deletion of *Pparγ* leads to cardiac hypertrophy[26] while cardiac-restricted overexpression of *Pparγ* leads to dilated cardiomyopathy associated with sudden death in young adulthood.[27] Homozygous *Pparγ* mutant embryos die at midgestation[24] and cardiac defects, including ventricular septal defect and OFT defects, were observed but correlated with placental dysfunction that severely compromises maternal-fetal exchange functions leading to early embryonic lethality. We observed OFT defects in *Pparγ* conditional mutant embryos after deletion with *Mesp1* but not *Mef2c-AHF*-Cre, implying a role for PPARγ in early cardiac progenitor cells. Since the *Mesp1* lineage also contribute to extraembryonic mesoderm,[35] *Mesp1-Cre;Pparγ*$^{fl/fl}$ cardiac defects may alternatively result from an extraembryonic origin of *Pparγ* deficiency. However, cardiac defects observed in *Mesp1-Cre;Pparγ*$^{fl/fl}$ conditional embryos are milder than homozygous *Pparγ* mutant embryos that show severe myocardial defects by E9.5.[24] More recently single-cell transcriptomic profiling of early E6.5 to E8.5 mouse embryos, reveals that among *Mesp1*-expressing cells which represent almost 34% of the extraembryonic mesodermal cells, only 0.4% display *Pparγ* expression.[55] Moreover, our results were obtained with embryos maintained in culture indicating that indirect effects of placental PPARγ on OFT morphogenesis are unlikely. Our results thus suggest a direct role of *Pparγ* in early cardiac progenitor cells for normal OFT elongation, a crucial developmental step during arterial pole development.[9,56] Early pharmacological impairment of PPARγ activity or genetic deletion of *Pparγ* in cardiac mesodermal cells led to a reduction of *Sema3c*-progenitor cells in the SHF. This is consistent with a reduced contribution of SHF cells to the iOFT wall. Interestingly, CHIP-X Enrichment Analysis[57] has identified *Sema3c* together with *Cd36* as PPARγ targets in preadipocyte cells in mice.[58] Our results are supported by evidence that *Pparγ* may play a critical role in early cardiac commitment and differentiation.[59] Indeed, gene expression analysis of cardiac derivatives from precardiac MESP1 (mesoderm posterior 1)-progenitors in induced human embryonic stem cells identified *Pparγ* as being rapidly activated upon stem cell differentiation. Enrichment of *Pparα*, although less than *Pparγ*, in the iOFT,[12] suggests additional roles of other *Ppar* family members in OFT development. In particular, the phenotypic recovery of the OFT elongation defect observed between midgestation and fetal stages in *Mesp1-Cre;Pparγ*$^{fl/fl}$ conditional embryos may suggest a genetic compensation or transcriptional adaptation to *Pparγ* knockout by other candidate genes. However, our data demonstrate that neither *Pparα* nor *Pparδ* are involved in this compensatory function at E9.5. To date, *Pparα* has not been shown to be required for OFT development. Indeed, *Pparα* knockout mice display adult cardiac dysfunction with no cardiac malformation.[60,61]

The superior wall of the OFT and subaortic myocardium originate from a subpopulation of progenitors positioned anterior to future subpulmonary progenitor cells in the SHF. These cells are positive for a *Hes1*-enhancer trap transgene and negative for *Tbx1* and *Hoxb1* genetic lineages.[8,12] Our results reinforce and support evidence for early patterning of distinct OFT myocardial progenitors along the anterior-posterior axis. *Hes1*$^{-/-}$mutant embryos display an OFT elongation defect and OFT malformations.[14] However, a direct role of *Hes1* in the SHF was not addressed. Our analysis of *Hes1* conditional deletion in early cardiac mesoderm progenitors and anterior SHF mesoderm points to an early temporal window for HES1 function in the SHF for normal OFT formation, consistent with the regionalized expression of *Hes1* in the most anterior subpopulation of the SHF and evidence for temporally distinct populations of progenitor cells contributing to the developing heart.[62] The development of subaortic myocardium may thus result from early committed SHF progenitors that are labeled by the

Hes1-transgene and contribute to the sOFT elongation. This conclusion is consistent with recent evidence for temporally distinct contributions of *Mef2c-AHF-Cre* progenitor cells to subaortic and subpulmonary myocardium, although *Hes1* itself appears to be required before the activation of *Mef2c-AHF-Cre*.[21]

Hes1 is a target gene and effector of the NOTCH signaling pathway and deficient NOTCH signaling within SHF progenitors leads to OFT defects affecting SHF and neural crest cell contributions to the OFT[43] as well as progenitor cell proliferation.[45] Identification of active NOTCH signaling in the sOFT suggests that regional activation of the NOTCH/HES1 pathway in the SHF regulates subaortic myocardial progenitor deployment to the sOFT. Results from High et al[43] support this conclusion: the authors showed that specific inactivation of NOTCH activity in the SHF leads to cardiac malformations such as persistent truncus arteriosus or double outlet right ventricle due to alterations in influx of cardiac neural crest cells. However, an expanded *Sema3c* expression domain in the myocardial OFT wall of mutant hearts points to a reduced or absent subaortic myocardial domain. NOTCH signaling is directly related to human CHD resulting from perturbed Jagged1/NOTCH signaling in the SHF in Alagille syndrome and tetralogy of Fallot.[63–65] Moreover, the NOTCH1 locus is the most frequent site of genetic variants predisposing to non-syndromic tetralogy of Fallot.[66,67] Together with our results, this suggests that NOTCH signaling regulates OFT development by controlling the regional transcriptional identity of the OFT and specifically future subaortic myocardium.

We also found that future subaortic myocardium expresses high levels of the non-canonical NOTCH ligand DLK1. Our results showing that DLK1 increases N1ICD immunoreactivity and Hes1 expression in the OFT suggest that during early heart morphogenesis, DLK1 activates the NOTCH signaling pathway. Dlk1 regulation of Notch signaling is complex and seems to be context and cell type dependent. Indeed, diverse effects of DLK1 on Notch signaling have been described, and although some reports demonstrate that Dlk1 acts through alternative signaling pathways including the Akt (serine/threonine kinase) and MAPK/ERK (mitogen activated kinase protein/ extracellular regulated MAP kinase) pathways, conflicting evidence supports both activation and inactivation of the Notch pathway in different contexts.[68] Nevertheless, the fact that a previous report in the developing heart found that Dlk1 positively regulates Notch1 signaling is in agreement with our findings.[69] PPARγ is an early marker of adipogenesis and one of the most critical activators of the adipogenic transcriptional program. DLK1, also known as PREF1 is a marker of undifferentiated preadipocyte expression which sharply decreases during early adipogenesis (when *Pparγ* is expressed). We showed that through the activation of the NOTCH/HES1 pathway, DLK1 may act to inhibit *Pparγ* expression in the sOFT wall. Interestingly, recent studies have reinforced our results showing that *Notch1* haploinsufficiency leads to *Pparγ* overexpression following downregulation of *Hes1* and *Dlk1*.[70] Together with our results, this suggests that NOTCH signaling may be a mechanism by which DLK1 restricts *Pparγ* expression. The strikingly complementary expression patterns of *Dlk1* and *Pparγ* expression in sOFT and iOFT subdomains raises the possibility that PPARγ impacts lipid metabolism as progenitor cells transit to the OFT. This possibility will be addressed in future experiments.

In summary, our findings demonstrate for the first time that PPARγ signaling together with NOTCH/HES1 signaling are both required in cardiac progenitor cells for normal heart tube elongation and regulate complementary transcriptional subdomains in the arterial pole of the embryonic heart. In addition, our results suggest that Dlk1, a noncanonical NOTCH ligand, may be part of this process thus identifying a novel molecular pathway controlling arterial pole development. Our work thus unveils new insight into the molecular mechanisms involved in developmental abnormalities of the heart that may be relevant for future clinical benefits.

ARTICLE INFORMATION

Received January 11, 2022; revision received September 7, 2022; accepted September 14, 2022.

Affiliations

Aix Marseille University, CNRS UMR 7288, IBDM, Marseille, France (M.R., M.T.R., R.S., F.R., R.G.K.) and Aix Marseille Univ, INSERM, MMG, Marseille, France (M.T.R., F.R.).

Acknowledgments

We thank Linglin Xie (Department of Nutrition, Texas A&M University, United states) for sharing with us embryos displaying *Pparγ* conditional deletion.

Sources of Funding

This work was supported by the European Commission under the Marie Curie Initial Training Network CardioNet (ITN-2011-GA289600 CardioNet, Marie Curie, ITN), the Fondation pour la Recherche Médicale (DEQ20150331717, FTD20150532561), Leducq Foundation (Transatlantic Network of Excellence, 15CVD01) and the Agence Nationale de la Recherche (ANR-14-CE12-0012, ANR-18-CE13-0011, ANR-20-CE13-0029-01).

Disclosures

None.

Supplemental Materials

Supplemental Methods
Figures S1–S5
References [5,9,12,14,56,71–76]

REFERENCES

1. Kelly RG, Brown NA, Buckingham ME. The arterial pole of the mouse heart forms from Fgf10-expressing cells in pharyngeal mesoderm. *Dev Cell*. 2001;1:435–440. doi: 10.1016/s1534-5807(01)00040-5
2. Mjaatvedt CH, Nakaoka T, Moreno-Rodriguez R, Norris RA, Kern MJ, Eisenberg CA, Turner D, Markwald RR. The outflow tract of the heart is recruited from a novel heart-forming field. *Dev Biol*. 2001;238:97–109. doi: 10.1006/dbio.2001.0409

3. Kelly RG. The second heart field. *Curr Top Dev Biol.* 2012;100:33–65. doi: 10.1016/B978-0-12-387786-4.00002-6
4. Buckingham M, Meilhac S, Zaffran S. Building the mammalian heart from two sources of myocardial cells. *Nat Rev Genet.* 2005;6:826–835. doi: 10.1038/nrg1710
5. De Bono C, Thellier C, Bertrand N, Sturny R, Jullian E, Cortes C, Stefanovic S, Zaffran S, Théveniau-Ruissy M, Kelly RG. T-box genes and retinoic acid signaling regulate the segregation of arterial and venous pole progenitor cells in the murine second heart field. *Hum Mol Genet.* 2018;27:3747–3760. doi: 10.1093/hmg/ddy266
6. Virani SS, Alonso A, Aparicio HJ, Benjamin EJ, Bittencourt MS, Callaway CW, Carson AP, Chamberlain AM, Cheng S, Delling FN, et al; American Heart Association Council on Epidemiology and Prevention Statistics Committee and Stroke Statistics Subcommittee. Heart disease and stroke statistics-2021 update: a report from the american heart association. *Circulation.* 2021;143:e254–e743. doi: 10.1161/CIR.0000000000000950
7. Bruneau BG. The developmental genetics of congenital heart disease. *Nature.* 2008;451:943–948. doi: 10.1038/nature06801
8. Huynh T, Chen L, Terrell P, Baldini A. A fate map of Tbx1 expressing cells reveals heterogeneity in the second cardiac field. *Genesis.* 2007;45:470–475. doi: 10.1002/dvg.20317
9. Théveniau-Ruissy M, Dandonneau M, Mesbah K, Ghez O, Mattei MG, Miquerol L, Kelly RG. The del22q11.2 candidate gene Tbx1 controls regional outflow tract identity and coronary artery patterning. *Circ Res.* 2008;103:142–148. doi: 10.1161/CIRCRESAHA.108.172189
10. Bajolle F, Zaffran S, Meilhac SM, Dandonneau M, Chang T, Kelly RG, Buckingham ME. Myocardium at the base of the aorta and pulmonary trunk is prefigured in the outflow tract of the heart and in subdomains of the second heart field. *Dev Biol.* 2008;313:25–34. doi: 10.1016/j.ydbio.2007.09.023
11. Bertrand N, Roux M, Ryckebüsch L, Niederreither K, Dollé P, Moon A, Capecchi M, Zaffran S. Hox genes define distinct progenitor subdomains within the second heart field. *Dev Biol.* 2011;353:266–274. doi: 10.1016/j.ydbio.2011.02.029
12. Rana MS, Théveniau-Ruissy M, De Bono C, Mesbah K, Francou A, Rammah M, Domínguez JN, Roux M, Laforest B, Anderson RH, et al. Tbx1 coordinates addition of posterior second heart field progenitor cells to the arterial and venous poles of the heart. *Circ Res.* 2014;115:790–799. doi: 10.1161/CIRCRESAHA.115.305020
13. Stefanovic S, Laforest B, Desvignes JP, Lescroart F, Argiro L, Maurel-Zaffran C, Salgado D, Plaindoux E, De Bono C, Pazur K, et al. Hox-dependent coordination of mouse cardiac progenitor cell patterning and differentiation. *Elife.* 2020;9:e55124. doi: 10.7554/eLife.55124
14. Rochais F, Dandonneau M, Mesbah K, Jarry T, Mattei MG, Kelly RG. Hes1 is expressed in the second heart field and is required for outflow tract development. *PLoS One.* 2009;4:e6267. doi: 10.1371/journal.pone.0006267
15. Lescroart F, Kelly RG, Le Garrec JF, Nicolas JF, Meilhac SM, Buckingham M. Clonal analysis reveals common lineage relationships between head muscles and second heart field derivatives in the mouse embryo. *Development.* 2010;137:3269–3279. doi: 10.1242/dev.050674
16. Lescroart F, Mohun T, Meilhac SM, Bennett M, Buckingham M. Lineage tree for the venous pole of the heart: clonal analysis clarifies controversial genealogy based on genetic tracing. *Circ Res.* 2012;111:1313–1322. doi: 10.1161/CIRCRESAHA.112.271064
17. Maeda J, Yamagishi H, McAnally J, Yamagishi C, Srivastava D. Tbx1 is regulated by forkhead proteins in the secondary heart field. *Dev Dyn.* 2006;235:701–710. doi: 10.1002/dvdy.20686
18. Goddeeris MM, Schwartz R, Klingensmith J, Meyers EN. Independent requirements for Hedgehog signaling by both the anterior heart field and neural crest cells for outflow tract development. *Development.* 2007;134:1593–1604. doi: 10.1242/dev.02824
19. Hoffmann AD, Peterson MA, Friedland-Little JM, Anderson SA, Moskowitz IP. sonic hedgehog is required in pulmonary endoderm for atrial septation. *Development.* 2009;136:1761–1770. doi: 10.1242/dev.034157
20. Sinha T, Lin L, Li D, Davis J, Evans S, Wynshaw-Boris A, Wang J. Mapping the dynamic expression of Wnt11 and the lineage contribution of Wnt11-expressing cells during early mouse development. *Dev Biol.* 2015;398:177–192. doi: 10.1016/j.ydbio.2014.11.005
21. Jin H, Wang H, Li J, Yu S, Xu M, Qiu Z, Xia M, Zhu J, Feng Q, Xie J, et al. Differential contribution of the two waves of cardiac progenitors and their derivatives to aorta and pulmonary artery. *Dev Biol.* 2019;450:82–89. doi: 10.1016/j.ydbio.2019.03.019
22. Michalik L, Desvergne B, Dreyer C, Gavillet M, Laurini RN, Wahli W. PPAR expression and function during vertebrate development. *Int J Dev Biol.* 2002;46:105–114.
23. Tontonoz P, Hu E, Spiegelman BM. Stimulation of adipogenesis in fibroblasts by PPAR gamma 2, a lipid-activated transcription factor. *Cell.* 1994;79:1147–1156. doi: 10.1016/0092-8674(94)90006-x
24. Barak Y, Nelson MC, Ong ES, Jones YZ, Ruiz-Lozano P, Chien KR, Koder A, Evans RM. PPAR gamma is required for placental, cardiac, and adipose tissue development. *Mol Cell.* 1999;4:585–595. doi: 10.1016/s1097-2765(00)80209-9
25. Finck BN. The PPAR regulatory system in cardiac physiology and disease. *Cardiovasc Res.* 2007;73:269–277. doi: 10.1016/j.cardiores.2006.08.023
26. Duan SZ, Ivashchenko CY, Russell MW, Milstone DS, Mortensen RM. Cardiomyocyte-specific knockout and agonist of peroxisome proliferator-activated receptor-gamma both induce cardiac hypertrophy in mice. *Circ Res.* 2005;97:372–379. doi: 10.1161/01.RES.0000179226.34112.6d
27. Son NH, Park TS, Yamashita H, Yokoyama M, Huggins LA, Okajima K, Homma S, Szabolcs MJ, Huang LS, Goldberg IJ. Cardiomyocyte expression of PPARgamma leads to cardiac dysfunction in mice. *J Clin Invest.* 2007;117:2791–2801. doi: 10.1172/JCI30335
28. Morrow JP, Katchman A, Son NH, Trent CM, Khan R, Shiomi T, Huang H, Amin V, Lader JM, Vasquez C, et al. Mice with cardiac overexpression of peroxisome proliferator-activated receptor γ have impaired repolarization and spontaneous fatal ventricular arrhythmias. *Circulation.* 2011;124:2812–2821. doi: 10.1161/CIRCULATIONAHA.111.056309
29. Yamaguchi Y, Cavallero S, Patterson M, Shen H, Xu J, Kumar SR, Sucov HM. Adipogenesis and epicardial adipose tissue: a novel fate of the epicardium induced by mesenchymal transformation and PPARγ activation. *Proc Natl Acad Sci U S A.* 2015;112:2070–2075. doi: 10.1073/pnas.1417232112
30. Ishibashi M, Ang SL, Shiota K, Nakanishi S, Kageyama R, Guillemot F. Targeted disruption of mammalian hairy and enhancer of split homolog-1 (HES-1) leads to up-regulation of neural helix-loop-helix factors, premature neurogenesis, and severe neural tube defects. *Genes Dev.* 1995;9:3136–3148. doi: 10.1101/gad.9.24.3136
31. Jerome LA, Papaioannou VE. DiGeorge syndrome phenotype in mice mutant for the T-box gene, Tbx1. *Nat Genet.* 2001;27:286–291. doi: 10.1038/85845
32. He W, Barak Y, Hevener A, Olson P, Liao D, Le J, Nelson M, Ong E, Olefsky JM, Evans RM. Adipose-specific peroxisome proliferator-activated receptor gamma knockout causes insulin resistance in fat and liver but not in muscle. *Proc Natl Acad Sci U S A.* 2003;100:15712–15717. doi: 10.1073/pnas.2536828100
33. Kita A, Imayoshi I, Hojo M, Kitagawa M, Kokubu H, Ohsawa R, Ohtsuka T, Kageyama R, Hashimoto N. Hes1 and Hes5 control the progenitor pool, intermediate lobe specification, and posterior lobe formation in the pituitary development. *Mol Endocrinol.* 2007;21:1458–1466. doi: 10.1210/me.2007-0039
34. Verzi MP, McCulley DJ, De Val S, Dodou E, Black BL. The right ventricle, outflow tract, and ventricular septum comprise a restricted expression domain within the secondary/anterior heart field. *Dev Biol.* 2005;287:134–145. doi: 10.1016/j.ydbio.2005.08.041
35. Saga Y, Miyagawa-Tomita S, Takagi A, Kitajima S, Miyazaki Ji, Inoue T. MesP1 is expressed in the heart precursor cells and required for the formation of a single heart tube. *Development.* 1999;126:3437–3447. doi: 10.1242/dev.126.15.3437
36. Srinivas S, Watanabe T, Lin CS, William CM, Tanabe Y, Jessell TM, Costantini F. Cre reporter strains produced by targeted insertion of EYFP and ECFP into the ROSA26 locus. *BMC Dev Biol.* 2001;1:4. doi: 10.1186/1471-213x-1-4
37. Iso T, Kedes L, Hamamori Y. HES and HERP families: multiple effectors of the Notch signaling pathway. *J Cell Physiol.* 2003;194:237–255. doi: 10.1002/jcp.10208
38. van Bueren KL, Papangeli I, Rochais F, Pearce K, Roberts C, Calmont A, Szumska D, Kelly RG, Bhattacharya S, Scambler PJ. Hes1 expression is reduced in Tbx1 null cells and is required for the development of structures affected in 22q11 deletion syndrome. *Dev Biol.* 2010;340:369–380. doi: 10.1016/j.ydbio.2010.01.020
39. Herzig S, Hedrick S, Morantte I, Koo SH, Galimi F, Montminy M. CREB controls hepatic lipid metabolism through nuclear hormone receptor PPAR-gamma. *Nature.* 2003;426:190–193. doi: 10.1038/nature02110
40. Maniati E, Bossard M, Cook N, Candido JB, Emami-Shahri N, Nedospasov SA, Balkwill FR, Tuveson DA, Hagemann T. Crosstalk between the canonical NF-κB and Notch signaling pathways inhibits Pparγ expression and promotes pancreatic cancer progression in mice. *J Clin Invest.* 2011;121:4685–4699. doi: 10.1172/JCI45797
41. Kitagawa M. Notch signalling in the nucleus: roles of Mastermind-like (MAML) transcriptional coactivators. *J Biochem.* 2016;159:287–294. doi: 10.1093/jb/mvv123

42. Luxán G, D'Amato G, MacGrogan D, de la Pompa JL. Endocardial Notch Signaling in Cardiac Development and Disease. *Circ Res*. 2016;118:e1–e18. doi: 10.1161/CIRCRESAHA.115.305350
43. High FA, Jain R, Stoller JZ, Antonucci NB, Lu MM, Loomes KM, Kaestner KH, Pear WS, Epstein JA. Murine Jagged1/Notch signaling in the second heart field orchestrates Fgf8 expression and tissue-tissue interactions during outflow tract development. *J Clin Invest*. 2009;119:1986–1996. doi: 10.1172/JCI38922
44. Eley L, Alqahtani AM, MacGrogan D, Richardson RV, Murphy L, Salguero-Jimenez A, Sintes Rodriguez San Pedro M, Tiurma S, McCutcheon L, Gilmore A, et al. A novel source of arterial valve cells linked to bicuspid aortic valve without raphe in mice. *Elife*. 2018;7:e34110. doi: 10.7554/eLife.34110
45. De Zoysa P, Liu J, Toubat O, Choi J, Moon A, Gill PS, Duarte A, Sucov HM, Kumar SR. Delta-like ligand 4-mediated Notch signaling controls proliferation of second heart field progenitor cells by regulating Fgf8 expression. *Development*. 2020;147:dev185249. doi: 10.1242/dev.185249
46. Gulyaeva O, Nguyen H, Sambeat A, Heydari K, Sul HS. Sox9-Meis1 inactivation is required for adipogenesis, advancing Pref-1+ to PDGFRα+ cells. *Cell Rep*. 2018;25:1002–1017.e4. doi: 10.1016/j.celrep.2018.09.086
47. Hao JW, Wang J, Guo H, Zhao YY, Sun HH, Li YF, Lai XY, Zhao N, Wang X, Xie C. et al. CD36 facilitates fatty acid uptake by dynamic palmitoylation-regulated endocytosis. *Nat Commun*. 2020; 11:1–16. doi: 10.1038/s41467-020-18565-8
48. Choi H, Lee H, Kim TH, Kim HJ, Lee YJ, Lee SJ, Yu JH, Kim D, Kim KS, Park SW, et al. G0/G1 switch gene 2 has a critical role in adipocyte differentiation. *Cell Death Differ*. 2014;21:1071–1080. doi: 10.1038/cdd.2014.26
49. Tontonoz P, Nagy L, Alvarez JG, Thomazy VA, Evans RM. PPARgamma promotes monocyte/macrophage differentiation and uptake of oxidized LDL. *Cell*. 1998;93:241–252. doi: 10.1016/s0092-8674(00)81575-5
50. Hondares E, Mora O, Yubero P, Rodriguez de la Concepción M, Iglesias R, Giralt M, Villarroya F. Thiazolidinediones and rexinoids induce peroxisome proliferator-activated receptor-coactivator (PGC)-1alpha gene transcription: an autoregulatory loop controls PGC-1alpha expression in adipocytes via peroxisome proliferator-activated receptor-gamma coactivation. *Endocrinology*. 2006;147:2829–2838. doi: 10.1210/en.2006-0070
51. Markan KR, Boland LK, King-McAlpin AQ, Claflin KE, Leaman MP, Kemerling MK, Stonewall MM, Amendt BA, Ankrum JA, Potthoff MJ. Adipose TBX1 regulates β-adrenergic sensitivity in subcutaneous adipose tissue and thermogenic capacity in vivo. *Mol Metab*. 2020;36:100965. doi: 10.1016/j.molmet.2020.02.008
52. Castellanos R, Xie Q, Zheng D, Cvekl A, Morrow BE. Mammalian TBX1 preferentially binds and regulates downstream targets via a tandem T-site repeat. *PLoS One*. 2014;9:e95151. doi: 10.1371/journal.pone.0095151
53. Bi P, Shan T, Liu W, Yue F, Yang X, Liang XR, Wang J, Li J, Carlesso N, Liu X, et al. Inhibition of Notch signaling promotes browning of white adipose tissue and ameliorates obesity. *Nat Med*. 2014;20:911–918. doi: 10.1038/nm.3615
54. Fulcoli FG, Franzese M, Liu X, Zhang Z, Angelini C, Baldini A. Rebalancing gene haploinsufficiency in vivo by targeting chromatin. *Nat Commun*. 2016;7:11688. doi: 10.1038/ncomms11688
55. Pijuan-Sala B, Griffiths JA, Guibentif C, Hiscock TW, Jawaid W, Calero-Nieto FJ, Mulas C, Ibarra-Soria X, Tyser RCV, Ho DLL, et al. A single-cell molecular map of mouse gastrulation and early organogenesis. *Nature*. 2019;566:490–495. doi: 10.1038/s41586-019-0933-9
56. Francou A, Saint-Michel E, Mesbah K, Kelly RG. TBX1 regulates epithelial polarity and dynamic basal filopodia in the second heart field. *Development*. 2014;141:4320–4331. doi: 10.1242/dev.115022
57. Lachmann A, Xu H, Krishnan J, Berger SI, Mazloom AR, Ma'ayan A. ChEA: transcription factor regulation inferred from integrating genome-wide ChIP-X experiments. *Bioinformatics*. 2010;26:2438–2444. doi: 10.1093/bioinformatics/btq466
58. Lefterova MI, Steger DJ, Zhuo D, Qatanani M, Mullican SE, Tuteja G, Manduchi E, Grant GR, Lazar MA. Cell-specific determinants of peroxisome proliferator-activated receptor gamma function in adipocytes and macrophages. *Mol Cell Biol*. 2010;30:2078–2089. doi: 10.1128/MCB.01651-09
59. den Hartogh SC, Wolstencroft K, Mummery CL, Passier R. A comprehensive gene expression analysis at sequential stages of in vitro cardiac differentiation from isolated MESP1-expressing-mesoderm progenitors. *Sci Rep*. 2016;6:19386. doi: 10.1038/srep19386
60. Lee SS, Pineau T, Drago J, Lee EJ, Owens JW, Kroetz DL, Fernandez-Salguero PM, Westphal H, Gonzalez FJ. Targeted disruption of the alpha isoform of the peroxisome proliferator-activated receptor gene in mice results in abolishment of the pleiotropic effects of peroxisome proliferators. *Mol Cell Biol*. 1995;15:3012–3022. doi: 10.1128/MCB.15.6.3012
61. Watanabe K, Fujii H, Takahashi T, Kodama M, Aizawa Y, Ohta Y, Ono T, Hasegawa G, Naito M, Nakajima T, et al. Constitutive regulation of cardiac fatty acid metabolism through peroxisome proliferator-activated receptor alpha associated with age-dependent cardiac toxicity. *J Biol Chem*. 2000;275:22293-9 - 10.1074/jbc.M000248200
62. Lescroart F, Chabab S, Lin X, Rulands S, Paulissen C, Rodolosse A, Auer H, Achouri Y, Dubois C, Bondue A, et al. Early lineage restriction in temporally distinct populations of Mesp1 progenitors during mammalian heart development. *Nat Cell Biol*. 2014;16:829–840. doi: 10.1038/ncb3024
63. Li L, Krantz ID, Deng Y, Genin A, Banta AB, Collins CC, Qi M, Trask BJ, Kuo WL, Cochran J, et al. Alagille syndrome is caused by mutations in human Jagged1, which encodes a ligand for Notch1. *Nat Genet*. 1997;16:243–251. doi: 10.1038/ng0797-243
64. McDaniell R, Warthen DM, Sanchez-Lara PA, Pai A, Krantz ID, Piccoli DA, Spinner NB. NOTCH2 mutations cause alagille syndrome, a heterogeneous disorder of the notch signaling pathway. *Am J Hum Genet*. 2006;79:169–173. doi: 10.1086/505332
65. Garg V, Muth AN, Ransom JF, Schluterman MK, Barnes R, King IN, Grossfeld PD, Srivastava D. Mutations in NOTCH1 cause aortic valve disease. *Nature*. 2005;437:270–274. doi: 10.1038/nature03940
66. Page DJ, Miossec MJ, Williams SG, Monaghan RM, Fotiou E, Cordell HJ, Sutcliffe L, Topf A, Bourgey M, Bourque G, et al. Whole exome sequencing reveals the major genetic contributors to nonsyndromic tetralogy of fallot. *Circ Res*. 2019;124:553–563. doi: 10.1161/CIRCRESAHA.118.313250
67. Manshaei R, Merico D, Reuter MS, Engchuan W, Mojarad BA, Chaturvedi R, Heung T, Pellecchia G, Zarrei M, Nalpathamkalam T, et al. Genes and pathways implicated in tetralogy of fallot revealed by ultra-rare variant burden analysis in 231 genome sequences. *Front Genet*. 2020;11:957. doi: 10.3389/fgene.2020.00957
68. Pittaway JFH, Lipsos C, Mariniello K, Guasti L. The role of delta-like non-canonical Notch ligand 1 (DLK1) in cancer. *Endocr Relat Cancer*. 2021;28:R271–R287. doi: 10.1530/ERC-21-0208
69. Shamis Y, Cullen DE, Liu L, Yang G, Ng SF, Xiao L, Bell FT, Ray C, Takikawa S, Moskowitz IP, et al. Maternal and zygotic Zfp57 modulate NOTCH signaling in cardiac development. *Proc Natl Acad Sci U S A*. 2015;112:E2020–E2029. doi: 10.1073/pnas.1415541112
70. Yamaguchi K, Hayashi M, Uchida Y, Cheng XW, Nakayama T, Matsushita T, Murohara T and Takeshita K. Notch1 haploinsufficiency in mice accelerates adipogenesis. *Sci Rep*. 2021;11:16761 - 10.1038/s41598-021-96017-z
71. Mesbah K, Rana MS, Francou A, van Duijvenboden K, Papaioannou VE, Moorman AF, Kelly RG, Christoffels VM. Identification of a Tbx1/Tbx2/Tbx3 genetic pathway governing pharyngeal and arterial pole morphogenesis. *Hum Mol Genet*. 2012;21:1217–1229. doi: 10.1093/hmg/ddr553
72. Lakkis MM, Epstein JA. Neurofibromin modulation of ras activity is required for normal endocardial-mesenchymal transformation in the developing heart. *Development*. 1998;125:4359–4367. doi: 10.1242/dev.125.22.4359
73. Schmittgen TD, Livak KJ. Analyzing real-time PCR data by the comparative C(T) method. *Nat Protoc*. 2008;3:1101–1108. doi: 10.1038/nprot.2008.73
74. Shapiro SS, Wilk MB. An analysis of variance test for normality (Complete Samples). *Biometrika*. 1965;52:591–611. doi: 10.2307/2333709
75. Faul F, Erdfelder E, Lang AG, Buchner A. G*Power 3: a flexible statistical power analysis program for the social, behavioral, and biomedical sciences. *Behav Res Methods*. 2007;39:175–191. doi: 10.3758/bf03193146
76. Faul F, Erdfelder E, Buchner A, Lang AG. Statistical power analyses using G*Power 3.1: tests for correlation and regression analyses. *Behav Res Methods*. 2009;41:1149–1160. doi: 10.3758/BRM.41.4.1149